Nonlinear Switching Filter for Color Image Filtering

BY

SUIHONG DENG

A Thesis submitted to
the Faculty of Graduate Studies
In Partial Fulfillment of the Requirements for the Degree of

MASTER OF SCIENCE

Department of Electrical and Computer Engineering
University of Manitoba
Winnipeg, Manitoba

The Faculty of Graduate Studies
500 University Centre, University of Manitoba
Winnipeg, Manitoba R3T 2N2

Phone: (204) 474 9377
Fax: (204) 474 7553
graduate_studies@umanitoba.ca

THE UNIVERSITY OF MANITOBA

FACULTY OF GRADUATE STUDIES

*****

COPYRIGHT PERMISSION

"Nonlinear Switching Filter for Color Image Filtering"

BY

Suihong Deng

A Thesis/Practicum submitted to the Faculty of Graduate Studies of The University of Manitoba in partial fulfillment of the requirement of the degree

Of

MASTER OF SCIENCE

Contents

List of Figures

List of Tables

Acknowledgement

I would like to express my deep and sincere gratitude to my advisor, Professor Miroslaw Pawlak. This work would not have been possible without his guidance. His wise knowledge, constructive suggestions built up a solid base for the present thesis, and guided me through the difficulties during the work.

I wish to thank my parents for their encouragement and support for my study all the time. I also want to thank my brother James and my sister-in-law Katherine. James gave many valuable comments on my thesis. Katherine helped me a lot to quickly accustom to the life in Canada. The warmth and happiness that I enjoyed so much with their family will definitely become part of my most precious memory in the future.

Abstract

Switch Filter is a conceptually simple but effective noise suppression filter. It has been demonstrated, by many researchers, that the switch filter can remove impulsive noise while preserving image details for greyscale image. In this work, this nonlinear filter is extended to process color image with both Mean Filter and Vector Median Filter incorporated in the framework for noise detection. The $L^*a^*b^*$ color space is selected as a perceptually uniform color space, which is a suitable model for Switch Filter to detect noise by comparing color difference. The conversion between the $L^*a^*b^*$ color space and the traditional RGB color space is nonlinear, which results in the dependence of the noise variance on the mean level. To preserve the property of noise, a variance stabilization transformation is derived. Extensive simulation studies demonstrate that such filter structure has a better performance than Sigma Filter when dealing with impulsive noise and a comparable output for the case of Gaussian noise.

Chapter 1 Introduction

1.1 Background

Noise removal filtering is one of the most fundamental research topics in image processing. Noise is unavoidable during image acquisition and image transmission. The image sensor is affected by a variety factors such as the temperature, the environmental conditions, and the quality of the sensor. Also, the channel interference is the principal source of noise during image transmission. To recover the noise-corrupted image to its "ideal" condition is an important and necessary pre-image processing step before any other image operations, such as segmentation, enhancement, and classification can be performed.

Image, as the reflection of the real world, contains abrupt changes or discontinuities to describe the shape of the objects. Thus, maintaining the sharpness of the edges is as important as removing the noise in the image. The traditional linear filters, the Wiener filter and the Gaussian low-pass filter as an example, usually smooth out the noise values with the expense of blurring the image, which results in the reduction of the image quality and the limitations for further image operations. For greyscale images, many efforts have been devoted to reducing this undesired side effect. A large class of nonlinear filters stemming from the theory of vertical weighting [1] [2], order statistics [3], and vector quantization [4] have been proposed.

The environment around human being is full of color features, and the perception of color is of paramount important to be used by human to recognize objects and collect information. In the last three decades, with the rapid development of the computation

power of computers, colors are becoming increasingly cheaper and easier to be generated and displayed, the use of color turns out to be more and more essential in the applications of computer vision and digital image processing.

Although a lot of noise removal algorithms have been developed for grey level image processing, it is essential to extend and/or reformulate them to process color image with the understanding of the mechanisms of color vision and the properties of color space. Applying the noise reduction methods developed for greyscale image directly to color image, like processing color channels separately, may be inappropriate due to unexpected color artefacts introduced. Therefore, the transition of these greyscale techniques to color image processing has to consider the correlations among the color channels. Vector value is treated in color image processing instead of the scalar data in greyscale image and algebraic ordering is used to compute the output signal. However, there is no universal method to order multivariate data. A number of ordering techniques have been proposed for various applications, which includes marginal ordering, reduced ordering, partial ordering, and conditional ordering. So far, some nonlinear multivariate filtering schemes have been proposed mainly based on reduced ordering [3]. Like their scalar counterparts, nonlinear filters have good non-Gaussian noise suppression and important image information preservation properties.

A color model is a mathematical specification of spectral colors in a finite dimensional vector space to efficiently specify, manipulate, and display the color objects taken into consideration. Nowadays, a number of color specification models for various applications are in use to preserve essential information and provide insight to what visual operations are needed; namely RGB, YIQ, HIS, XYZ, $L^*u^*v^*$ and $L^*a^*b^*$, the latter two

are perceptually uniform color spaces standardized by CIE (Commission Internationale de l'Eclairage or the International Commission on Illumination).

In my thesis, a new nonlinear approach for color image denoising is presented. It belongs to the group of filters stemming from the concept of switch scheme described in [5]. The proposed filters not only preserve edges and details in color images as its original form does in monochrome images, but also have an excellent performance in preserving the color consistency when the color space properly chosen. With the assumption of the additive noise model, a discussion about variance stabilization transformation to preserve the additivity of noise is also presented because a nonlinear conversion between two color spaces occurs.

1.2 Structure of thesis

The rest of the thesis is organized as follows.

Chapter 2 discusses mean filter and median filter as the typical type of linear filter and nonlinear filter, respectively, and describes the scheme of switch filter. It also gives a brief review of the sigma filter.

Chapter 3 describes the variable stabilization transformation utilized on the switch filter after converting the image signal from RGB space to $L^*a^*b^*$ space, in order to maintain the additivity of noise, while the color models used in the proposed filter are also concisely introduced.

Chapter 4 presents the simulation results of the switch scheme in comparison of the sigma filter processing color images corrupted by additive noise.

Chapter 5 summarizes the switch filter schemes as well as the future work to improve the performance of the switch filters.

Chapter 2 Preliminaries and the Proposed Filter Scheme

2.1 Noise Model

Due to image sensors' performance and/or the transmission interference, the color images are often contaminated by noise. Gaussian noise and impulsive noise are the two most frequently used noise models to characterize the corruption process.

In many practical applications, if there is error during image transmission or introduced by malfunctions of the image sensor, the pixel value of the image will become larger compared with the strength of the image signal. The multivariate impulsive model is used to simulate this kind of noise. For color image in RGB space, we assume that the additive noise is independent from pixel to pixel and uncorrelated among color components. The noise model can be written as,

$$\tilde{f}_{\mathrm{Im}\,pulsive}(x_i)=\begin{cases}(f_r(x_i),f_g(x_i),f_b(x_i)) & \text{with probability } (1-p)\\ (f_r(x_i)+d,f_g(x_i),f_b(x_i)) & \text{with probability } p_1\\ (f_r(x_i),f_g(x_i)+d,f_b(x_i)) & \text{with probability } p_2\\ (f_r(x_i),f_g(x_i),f_b(x_i)+d) & \text{with probability } p_3\\ (f_r(x_i)+d,f_g(x_i)+d,f_b(x_i)) & \text{with probability } p_4\\ (f_r(x_i)+d,f_g(x_i),f_b(x_i)+d) & \text{with probability } p_5\\ (f_r(x_i),f_g(x_i)+d,f_b(x_i)+d) & \text{with probability } p_6\\ (f_r(x_i)+d,f_g(x_i)+d,f_b(x_i)+d) & \text{with probability } p_7\end{cases} \tag{2.1}$$

where $\tilde{f}_{\mathrm{Im}\,pulsive}(x_i)$ denotes the noisy signal, $f(x_i)=(f_R(x_i),f_G(x_i),f_B(x_i))$ is the noise-free color vector, $\sum_{i=1}^{7} p_i = p$, and d can have either positive or negative values with the same probability to indicate the noise impulse height. If the corrupted value goes

outside the range of the color model, it will be mapped to one of the endpoints of the integer range specified by the 8-bit arithmetic.

For the case of noise produced during image generation, it is reasonable to model such noise as zero mean Gaussian noise with the assumption that it's independent and identically distributed, the model is written as,

$$\tilde{f}_{Gaussian}(x_i) = f(x_i) + \varepsilon(x_i), \tag{2.2}$$

where $f(x_i)$ is the noise free color signal and $\varepsilon(x_i) = (\varepsilon_r(x_i), \varepsilon_g(x_i), \varepsilon_b(x_i))$ is the Gaussian noise vector with no correlation among three color channels. Hence, the probability density function of the noise is:

$$p(\varepsilon_r) = p(\varepsilon_g) = p(\varepsilon_b) = \frac{1}{\sqrt{2\pi}\sigma} e^{-\frac{\varepsilon_i^2}{2\sigma^2}}. \tag{2.3}$$

A mixed impulse and Gaussian noise model is also used in this thesis to simulate the situations when an image is corrupted by both additive Gaussian thermal noise and impulsive transmission noise.

$$\tilde{f}_{Mixed}(x_i) = \begin{cases} \tilde{f}_{\text{Im }pulsive}(x_i) & \text{with probability } p \\ \tilde{f}_{Gaussian}(x_i) & \text{otherwise 1-}p \end{cases}, \tag{2.4}$$

where $\tilde{f}_{\text{Im }pulsive}(x_i)$ is the image signal corrupted by multivariate impulsive noise and $\tilde{f}_{Gaussian}(x_i)$ represents image signal corrupted by zero mean, white Gaussian noise.

2.2 Linear and Nonlinear Filters

Spatial filtering, computationally less expensive than the frequency filtering, is often chosen to deal with additive noises. The spatial filtering falls into two categories, linear filtering and non-linear filtering. For linear filtering, the implementation can be considered simply as weighted sum of pixels in the neighbourhood of the pixel being processed. One of the most attractive advantages of linear filters is that they can be efficiently implemented since the pixels can be processed in parallel. The classic mean filter is a typical linear filter with all weights equal to 1. A general definition of the mean filter is:

Definition. Let S_{x_i} represent the set of neighbourhood pixels in the rectangular window of size $m \times n$, centered at point x_i. The weighted mean filter computes a weighted average value of the pixels in the window.

$$\hat{f}(x_i) = \frac{1}{\sum_{x_j \in S_{x_j}} w(x_j)} \sum_{x_j \in S_{x_i}} w(x_j) \cdot f(x_j) \tag{2.5}$$

Based on the assumption of slow spatial variation in the image, the mean filter can restore the supposedly corrupted pixel value. However, at the edges this assumption fails, so the image is smeared by the averaging operation. To minimize the blurring side effect, local data information can be utilized to determine the weights. In greyscale image processing, for example, the Partition Weighted Sum Filter [4] uses Vector Quantization to optimize the weight for each partition observation space.

The extension of the mean filter to color image simply treats each color vector component separately and then combines the individual results together. Thus, similar blurring phenomenon occurs. To reduce the unacceptable effect, the mean filter can be combined with nonlinear techniques. The adaptive vector mean filter based on fuzzy logic principles [3] demonstrates a beautiful compromise of linear filter with nonlinear one. The output of the filter is calculated from the linear-combination of all pixels in the neighbourhood. However, the weighting of the pixels are determined by their similarity index with the central pixel. When the noise is unknown *a priori*, this type of filter performs well as general purpose filter, which means that it can not only preserve the mean filter's strong performance on Gaussian noise removal, but also improve the ability of smoothing impulsive noise.

Non-linear filters have some notable advantages over linear ones. For example, they outperform the linear filters especially in terms of image edge preserving. They also give satisfied results to suppress short tail noises. Order statistics filters are the most popular among this type of filters.

The median filter, which was first introduced by Tukey [6] [7], along with its modifications, attracted most attentions among a large number of nonlinear filters. A generalized definition of median filter is:

Definition. Let S_{x_i} represent the set of neighbourhood pixels in the rectangular window of size $m \times n$, centered at point x_i. The median filter replaces the value of the center pixel with the median value of the pixels within this window associated with the integer weights.

$$\hat{f}(x_i) = \underset{x_j \in S_{x_i}}{Med}\{w(x_j) \Diamond f(x_j)\} \tag{2.6}$$

where ◊ denotes duplication. As a special case, when all weights are equal to one, this general formula is simplified as the classic median filter. Besides of the aforementioned merits of nonlinear filters, the median filter has an important feature that it always outputs one of the input values within the data window, which is useful for finding the root signal of the image.

For scalar data, the symmetry center of a distribution of data is its median. However, when this concept is generalized to higher dimension like color image, the multidimensional median can be estimated in several ways based on the definitions of symmetry. There are mainly four types of symmetry: points of spherical, elliptical, central and angular symmetry. [8]

The Vector Median Filter (VMF) [9] which employs the center of spherical symmetry as the median is the most popular median filter to process vector values. L_1 norm is utilized to quantify the distance between any two color pixels so that the vector values can be ordered by their relative magnitude differences. The vector $\hat{f}(x_i)$ is the output value of the VMF such that for all x in the neighbourhood,

$$\sum_{j=1}^{N} \left| \hat{f}(x_i) - f(x_j) \right| \leq \sum_{j=1}^{N} \left| f(x) - f(x_j) \right|.$$

2.3 Sigma Filter

The sigma filter was first proposed by Lee [1] [2] in order to remove image noise while preserving the edge details. In Gaussian distribution, the sigma probability is defined as that the probability of a random variable is within two standard deviations of its mean. Motivated by the sigma probability, Sigma Filter averages the pixel values not only

along the horizontal direction but also along the vertical direction, and compares the difference among the pixels values in the local neighbourhood window. Therefore, the closeness between two pixel values is considered in terms of both spatial location and greyscale difference. The sigma filter can be understood easily by considering it as a local weighted averaging filter.

With same assumption as made in previously session, the noise is considered as spatially independent, identically distributed and uncorrelated with respect to the original uncorrupted image itself. Therefore, the observation image is modeled as,

$$\tilde{f}(x_i) = f(x_i) + \varepsilon \qquad i = 1.....n$$

To recover the corrupted image $\tilde{f}(x_i)$, The sigma filter may be written in a common form as

$$\hat{f}(x_i) = \sum_{j=1}^{n} \omega_{i,j} \tilde{f}(x_j), \tag{2.7}$$

where the weights $\omega_{i,j}$ are

$$\omega_{i,j} = \frac{K_h(x_i - x_j) L_g(\tilde{f}(x_i) - \tilde{f}(x_j))}{\sum_{j'=1}^{n} K_h(x_i - x_{j'}) L_g(\tilde{f}(x_i) - \tilde{f}(x_{j'}))}. \tag{2.8}$$

In this equation, $K_h(\cdot) = (1/h)K(\cdot/h)$, and $L_g(\cdot) = (1/g)L(\cdot/g)$, are kernel functions to control the averaging amount in both horizontal and vertical directions, h and g are used to define the bandwidth of the kernel functions.

In the original sigma filter proposed by Lee, the sigma filter for monochrome image utilizes the uniform density function to generate the weighting. Further research was done

by [10] with the conclusion that standard Gaussian density $\frac{1}{\sqrt{2\pi}} e^{-\frac{x^2}{2}}$ for both kernel functions gave the best result.

However, when this filter is extended to process color images that use a three-variate vector to represent a pixel's color value, it brings up a question about how to determine the weighting for each pixel. Each color component of an image pixel is not separate information so that the reduced ordering technique for vector values is selected to generate the weighting. Since the Euclidean distance is a reasonable measurement to define the magnitude difference between any two colors, it's used in the extension of sigma filter for color image processing.

$$\|f(x)-f(\xi)\| = \sqrt{(\Delta R)^2+(\Delta G)^2+(\Delta B)^2} \tag{2.9}$$

The procedure of sigma filter is as following:

- Establish a spatial distance range h and a color distance range g.
- Determine the colour difference in terms of Euclidean distance between the pixel in the centre and the other pixels in the local window.
- Generate the weighting of each pixel using (2.8) based on the color difference computed in previous step.
- Output the estimated color image $\hat{f}(x)$ using (2.7) in R, G and B channel individually.

The standard Gaussian function is used for both kernel function $K_h(\cdot)$ and $L_g(\cdot)$.

2.4 The Switch Filter Scheme

A large number of noise removal filters have been proposed for the purpose of removing the noise while preserving the edges and subtle details, the switch filters [5] [11], as a big family among them, is first introduced as a remedy for Median filters which tend to wrongly detect the thin line details as noisy signal.

The idea of switch scheme is very simple. If the center pixel of the neighbourhood is determined to be corrupted by the noise, it's replaced by the filter output; otherwise it's considered to be a noise free pixel and the pixel value remains unmodified. The switch scheme can be applied as an expansion to any desirable filter. Both the mean switch filter and the median switch filter have been incorporated in this frame work in Chapter 4.

The detection of noise is implemented by an impulse detector. The magnitude difference between the pixel value in the center and the filter's output is utilized as the measurement for the impulse detector.

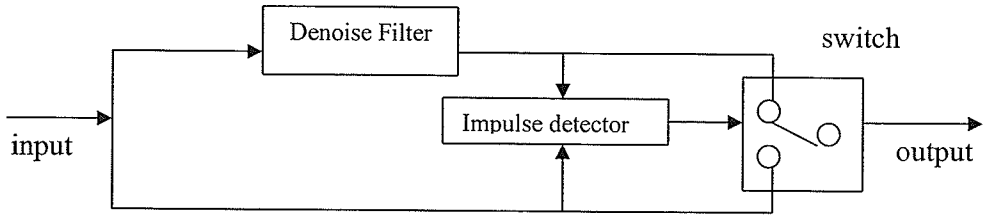

Fig. 2-1 Original Switch Filtering Scheme

In greyscale image processing, Let $f(x_i)$ and $\tilde{f}(x_i)$ represent the pixel value at position x_i in the original and corrupted image respectively. The output of the switch scheme within processing window at centre x_i is denoted by $\hat{f}(x_i)$. Detection of the noise can be implemented by the impulse detector. The detector measures the filter output $\bar{f}(x_i)$

with the input pixel $\tilde{f}(x_i)$. If the absolute difference between them exceeds a predefined threshold T, the pixel x_i is considered as a noisy one, $\bar{f}(x_i)$ is used to replace this noise corrupted pixel for restoration; otherwise the pixel is treated as noise free and its value is preserved. Therefore, the switch scheme is written as,

$$\alpha = \begin{cases} 1 & \left|\bar{f}(x_i) - \tilde{f}(x_i)\right| > T \\ 0 & \left|\bar{f}(x_i) - \tilde{f}(x_i)\right| \le T \end{cases}$$

$$\hat{f}(x_i) = \alpha \cdot \bar{f}(x_i) + (1-\alpha) \cdot \tilde{f}(x_i) \tag{2.9}$$

When utilizing in color image processing, switch scheme deals with vector data instead of scalar data. The α is extended to a matrix to specifically define the correlation between the input value and the filter output for every color component. This matrix is generally a diagonal one as only components with the same color has correlation. In my work, the diagonal elements are all set to 1.

By utilizing the switch scheme, one more parameter is taken into consideration, which is the threshold value T. When $T=0$, the switch filter performs identically as the filter employed in it, i.e. a median switch filter. It outputs the same result as the traditional median filter does and the threshold T doesn't have any effect. On the other hand, if T tends to be large enough to exceed the maximal range of the pixel value, there will be no modification made on the image, which means the switch filter is useless in this case. Therefore, the threshold value T should be chosen carefully to maximize the filter's effect. The computer simulation to derive a reasonable T for the filter will be conducted in Chapter 4.

When the switch scheme is applied to process multi-channel images, in order to yield a more accurate result of the color information, the noise removal filters operate in the $L^*a^*b^*$ color space which is a perceptually uniform color space, and the Euclidean distance can be used to quantify the color distance between the central pixel and the output of the noise removal filter. Because of the nonlinear transformation between RGB color space and $L^*a^*b^*$ color space, the preceding assumption of noise's additivity fails and the noise becomes signal dependent. Hence, a variance stabilisation transformation is employed to maintain the property of the noise models. A detailed discussion of color spaces and variance stabilization transformation will be presented in the following chapter. The proposed switch filter scheme is illustrated in Fig. 2-2.

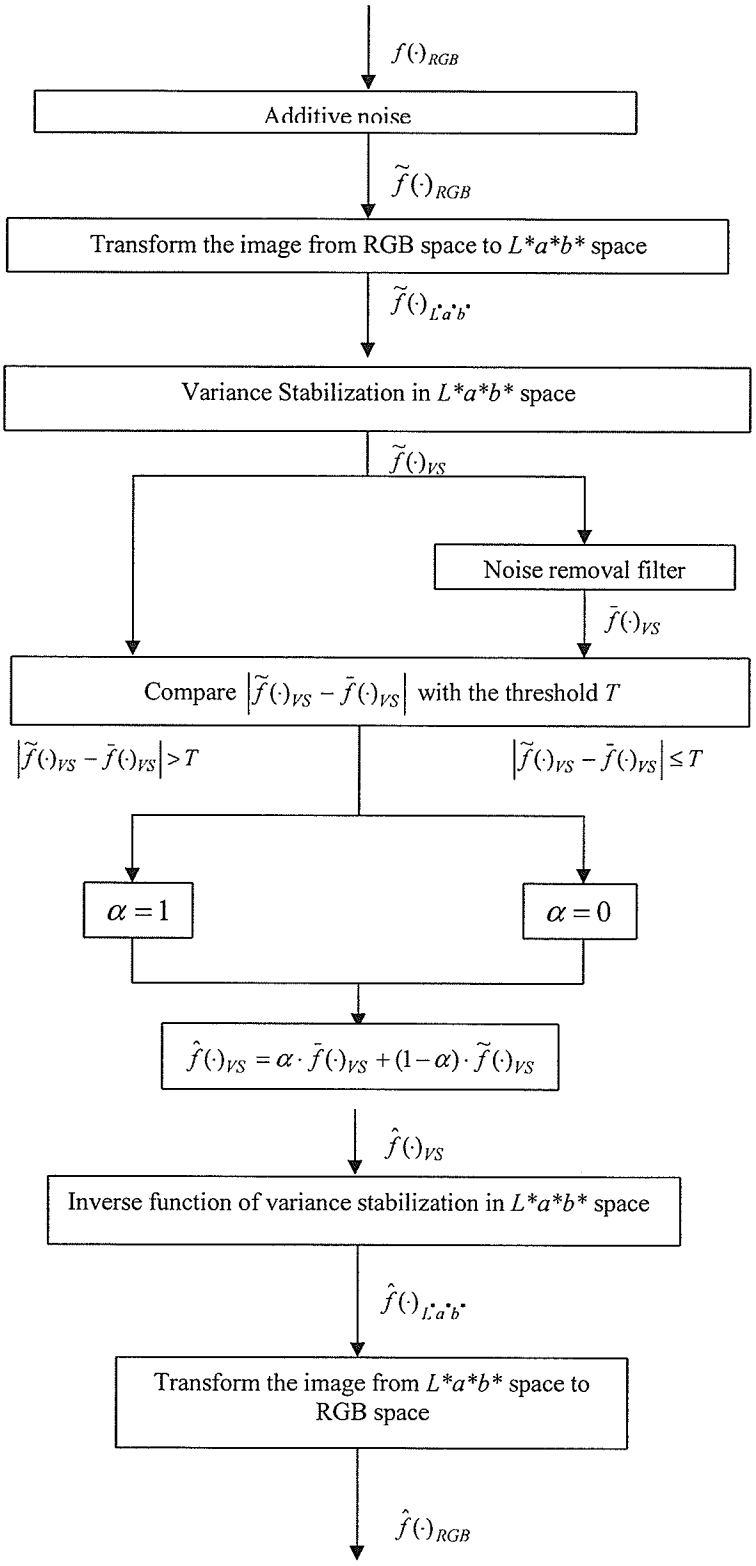

Fig. 2-2 The Switch Filter Scheme

Chapter 3 Color Spaces and Variance Stabilization

3.1 Color Spaces

The use of color in image processing becomes more and more popular due to two principal reasons. The first one is that color is a powerful descriptor that often simplifies object identification and extraction from a scene. Secondly, humans can distinguish thousands of colour shade and intensities, compared to only 256 shades of grey. Nowadays, with the digital revolution, color has become even more accessible. The techniques of color image processing have been tremendously developed. Color scanners, liquid crystal displays (LCD), digital cameras, and printers become an integral part of our everyday life.

3.1.1 Color Fundamentals

The study of color started from the experiment [10] of Sir Isaac Newton in 1666, which used a glass prism to dispel a beam of sunlight that passed through, and discovered that the white light consists of a continuous spectrum of colors ranging from violet at one end to red at the other. After the understanding of the nature of the color sensing system in human eyes, more knowledge about the color was discovered. Cones are the sensors in the eye responsible for color vision. Over 6 million cones in eye can be divided into three principal color receptors [12], approximately 65% cones are sensitive to red light, 33% to green lights, and the last 2% to blue lights (these blue cones are the most sensitive ones). From the research work of Grassmann [13] and Maxell [14], color can be mathematically

specified in terms of the three primary colors red (R), green (G), and blue (B). In 1931, the CIE established a standard for the three coordinates: blue = 435.8nm, green = 546.1nm, and red = 700 nm. With different combinations of these three primary colors, most color in the spectrum can be generated, although not all of them.

To utilize color in the applications of image processing, multimedia or computer vision, an appropriate color space is needed to rationally quantify colors in a finite dimensional vector space and provide crucial information for the visual operations.

3.1.2 RGB Color Space

This color space is the most straightforward one which is inspired by the structure of the human eyes. The three primary colors are red, green and blue. Each color in this space is presented as a mixture function of the primaries and the fraction of each primary that is mixed. A subspace in the RGB space consists of most of the colors that interest us, which we call it the cube. The cube is shown in Fig. 3-1. By assumption, this cube is

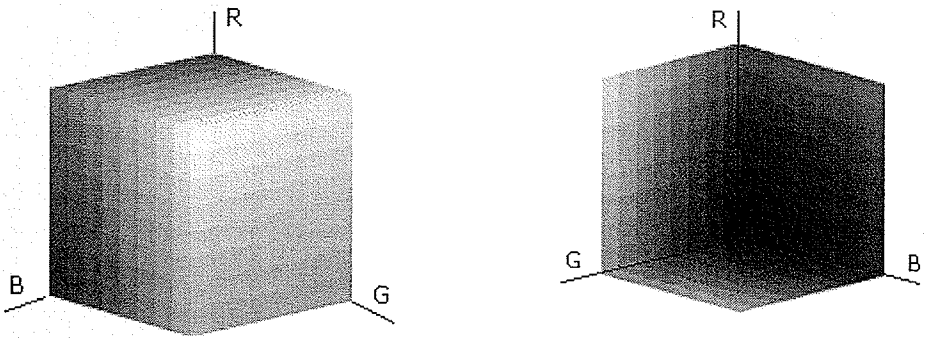

Figure 3-1The cube of RGB color space

normalized, that is, all values of R, G, B are in the range [0, 1]. The origin (0,0,0) of the cube corresponds to black; The corner farthest from the origin, defined as (1,1,1),

corresponds to white; The three corner on the coordinates are red, green and blue; The three other corners are cyan, magenta, and yellow. The diagonal line from the point (0,0,0) to the point (1,1,1) represents the levels of greyness from blackness to whiteness by itself. Other different colors are all on or inside this cube, which means that the cube is solid.

In image processing and multimedia video systems the RGB representation is the most often used. A digital color image can be represented by a two dimensional array of three channel vectors which consists of the pixel's red, green and blue values. Since this color model has an approximate relation to the human visual system which has a nonlinear perceptual response to intensity, it cannot be used for accurate perceptual computations.

3.1.3 CIE XYZ Color Space

The CIE XYZ color space standardized in 1931 is at the root of all colorimetry. It's a system based on the measurements of the color-matching abilities of the average human eye, in which all visible colors can be represented by positive values of the three primaries X, Y and Z. The Y primary represents luminance while X and Z carry the color information. The three primaries are assumed to be within the range [0, 1]. Besides that, the sum of X, Y and Z is equal to 1 for every color. Therefore, Z can be interpreted as a redundant coordinate and X and Y coordinates are sufficient to characterize this color space, as in Fig. 3-2.

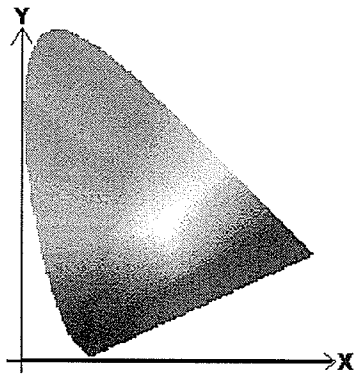

Figure 3-2 CIE XYZ color space representation on XY level area

Despite of the disadvantages that this color space is complex to implement and the color specified in XYZ terms is not user intuitive, CIE XYZ color space provides a useful bridge to convert between CIE values and between CIE and non-CIE color spaces. The conversion between XYZ space and RGB space is a linear transformation as shown as following,

$$\begin{bmatrix} X \\ Y \\ Z \end{bmatrix} = \begin{bmatrix} 0.4125 & 0.3576 & 0.1804 \\ 0.2127 & 0.7152 & 0.0722 \\ 0.0193 & 0.1192 & 0.9502 \end{bmatrix} \cdot \begin{bmatrix} R \\ G \\ B \end{bmatrix}. \tag{3.1}$$

3.1.4 *L*a*b** Color Space

It's natural to consider how to use the distance between any two colors in the 3-D color space to quantify the perceived difference between them. Unfortunately, most color spaces, including the aforementioned RGB and CIE XYZ color spaces, are not perceptually uniform. Equal perceptual difference between any colors does not correspond to equal distance in the tristimulus space. In 1976, CIE recommended two uniform color spaces for practical applications, one is the CIE $L^*u^*v^*$ and the other is CIE $L^*a^*b^*$ space. Both of these two spaces are derived based on the CIE XYZ space and white reference point.

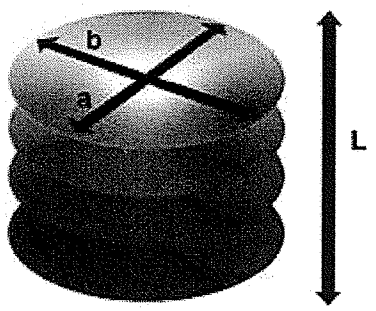

Figure 3-3 The L*a*b* Color Space

CIE $L^*a^*b^*$ space is composed by the perceived lightness axis and a set of opponent color axes, approximately red-green versus yellow-blue. The lightness scale L^* is used to determine the difference of light levels, L^*

is in the range [0, 100] with 0 corresponding to the black point and 100 to a white reference point. The chromaticity scale a^* and b^* represents the color changes from red to green and yellow to blue, respectively.

The L*, a*, b* values can be transformed from tristimulus value X, Y, Z of CIE XYZ color space according to the following formulae, given in [16]

$$\begin{aligned} L^* &= 116 g(\frac{y}{Y_n}) - 16 \\ a^* &= 500 \cdot (g(\frac{x}{X_n}) - g(\frac{y}{Y_n})) \\ b^* &= 200 \cdot (g(\frac{y}{Y_n}) - g(\frac{z}{Z_n})) \end{aligned} \tag{3.2}$$

where

$$g(x) = \begin{cases} x^{\frac{1}{3}} & x > 0.008856 \\ 7.787x + \dfrac{16}{116} & x \le 0.008856 \end{cases}$$

and X_n, Y_n, Z_n are constants which are the tristimuli of the white reference point.

Euclidean distances between two color stimuli in the CIE $L^*a^*b^*$ space provide a color difference measurement to evaluate color differences perceptually.

$$\Delta E^*_{Lab} = \sqrt{(\Delta L)^2 + (\Delta a)^2 + (\Delta b)^2} \tag{3.3}$$

This feature of CIE $L^*a^*b^*$ space is a magnificent advantage to keep the color information when using noise removal filters, it's a well suited color space to implement our proposed switch filters in.

3.2 Variance Stabilization

3.2.1 Variance Stabilization Transformation

Variance stabilization transformations have been used in statistical analysis to stabilize the variance. Some work with particular reference to analysis of variance had been reviewed and extended in [17] and [18]. If the variance tends to change with the mean level of the measurements, the variance will only be stabilized by a suitable transformation to change the scale of the data.

Principle of Variance Stabilization For any twice differentiable function $\phi(X)$, the random variable $Y = \phi(X)$ has variance σ_Y^2 which is (approximately) independent of μ_Y, and the transformed variable Y is said to have stable variance.

Suppose $Var(X) = \sigma_x^2(\mu)$ where μ is the mean of X and the transformation to stabilize the variance is $Y = \phi(X)$. Taylor's expansion gives first-order approximation,

$$\phi(X) \cong \phi(\mu) + (X - \mu) \cdot \phi'(\mu)$$

Since $E(X - \mu) = 0$, under this approximation, we have

$$E[\phi(X)] = \phi(\mu)$$

and

$$Var[\phi(X)] = E[\phi'(\mu) \cdot (X - \mu)]^2 = [\phi'(\mu)]^2 \sigma_x^2(\mu)$$

So, if we set

$$Var[\phi(X)] = c^2$$

where c is a positive constant, then

$$\phi(x) = c\int \frac{1}{\sigma_x(x)} dx$$

is the transformation to stabilize the variance.

3.2.1 The Derivation of the Transformation

When transforming image from RGB domain to $L^*a^*b^*$ domain or vice versa, the XYZ color space is used as a bridge. Although the transformation from RGB to XYZ is linear and the noise's additivity remains unchanged, the nonlinear transformation from XYZ space to $L^*a^*b^*$ space results in the signal dependence of the noise, which means its variance changes along with the mean level. To restore its additivity, a variance stabilization transformation is derived.

Assume the means of the three coordinates of an image in XYZ space are x_0, y_0, z_0, respectively, and the corresponding variances are $\sigma_x^2, \sigma_y^2, \sigma_z^2$.

The transformation that will be used to restore the additivity of the noise in the $L^*a^*b^*$ color space can be derived following the procedure described in previous session as,

$$\begin{cases} L_{VS} = \phi(L) = \dfrac{c}{(116)^3 \cdot \sigma_y}(L+16)^3 \\ a_{VS} = \phi(a) = k_1\left(\dfrac{1}{116}L + \dfrac{16}{116}\right)^3 a + k_2\left(\dfrac{1}{116}L + \dfrac{16}{116}\right)^4 \\ b_{VS} = \phi(b) = k_3\left(\dfrac{1}{116}L + \dfrac{16}{116}\right)^3 a + k_4\left(\dfrac{1}{116}L + \dfrac{16}{116}\right)^4 \end{cases}$$

Where c is a positive constant,

$$k_1 = \frac{3\cdot 116\cdot c\cdot X_n}{\sigma_x}\left[\begin{array}{l}\dfrac{1}{1500}-\dfrac{\sqrt{\sigma_y X_n}^{5}}{1000\sqrt{\sigma_x Y_n}^{5}}\ln\dfrac{\sqrt{\sigma_y X_n}-\sqrt{\sigma_x Y_n}}{\sqrt{\sigma_y X_n}+\sqrt{\sigma_x Y_n}}+\dfrac{\sqrt{\sigma_y X_n}^{2}\left(\sqrt{\sigma_y X_n}^{2}+\sqrt{\sigma_x Y_n}^{2}\right)}{2000\sqrt{\sigma_x Y_n}^{4}} \\ -\dfrac{\sqrt{\sigma_y X_n}^{2}}{2000\sqrt{\sigma_x Y_n}^{2}}\left(\dfrac{1}{3}+\dfrac{3\sqrt{\sigma_y X_n}^{2}}{\sqrt{\sigma_x Y_n}^{2}}\right)\end{array}\right]$$

$$k_2 = \frac{3\cdot 116\cdot c\cdot X_n}{\sigma_x}\left[\frac{1}{3}-\frac{\sqrt{\sigma_y X_n}}{8\sqrt{\sigma_x Y_n}}\left(1-\frac{\sqrt{\sigma_y X_n}^{4}}{\sqrt{\sigma_x Y_n}^{4}}\right)\ln\frac{\left(\sqrt{\sigma_y X_{n_0}}-\sqrt{\sigma_x Y_n}\right)}{\left(\sqrt{\sigma_y X_n}+\sqrt{\sigma_x Y_n}\right)}-\frac{\sqrt{\sigma_y X_n}^{2}}{4\sqrt{\sigma_x Y_n}^{2}}\left(\frac{1}{3}+\frac{\sqrt{\sigma_y X_n}^{2}}{\sqrt{\sigma_x Y_n}^{2}}\right)\right]$$

$$k_3 = \frac{3\cdot 116\cdot c\cdot Y_n}{\sigma_y}\left[\begin{array}{l}\dfrac{1}{600}-\dfrac{\sqrt{\sigma_y Z_n}^{3}}{400\sqrt{\sigma_z Y_n}^{3}}\ln\dfrac{\sqrt{\sigma_y Z_n}-\sqrt{\sigma_z Y_n}}{\sqrt{\sigma_y Z_n}+\sqrt{\sigma_z Y_n}}+\dfrac{\sqrt{\sigma_y Z_n}\left(\sqrt{\sigma_y Z_n}^{2}+\sqrt{\sigma_z Y_n}^{2}\right)}{800\sqrt{\sigma_z Y_n}^{3}} \\ -\dfrac{1}{800}\left(\dfrac{1}{3}+\dfrac{3\sqrt{\sigma_y Z_n}^{2}}{\sqrt{\sigma_z Y_n}^{2}}\right)\end{array}\right]$$

$$k_4 = -\frac{3\cdot 116\cdot c\cdot Y_n}{\sigma_y}\left[\frac{1}{3}+\frac{\sqrt{\sigma_y Z_n}}{2\sqrt{\sigma_z Y_n}}\left(1-\frac{\sqrt{\sigma_y Z_n}^{4}}{\sqrt{\sigma_z Y_n}^{4}}\right)\ln\frac{\left(\sqrt{\sigma_y Z_n}-\sqrt{\sigma_z Y_n}\right)}{\left(\sqrt{\sigma_y Z_n}+\sqrt{\sigma_z Y_n}\right)}-\frac{1}{4}\left(\frac{1}{3}+\frac{\sqrt{\sigma_y Z_n}^{2}}{\sqrt{\sigma_z Y_n}^{2}}\right)\right]$$

and X_n, Y_n, Z_n are constants which are the tristimuli of the white reference point.

The followings are the derivations of the transformation for three coordinates.

- **Derivation of Transformation for *L****

Firstly, the stabilization transformation for L^* coordinate is derived. The Taylor expansion of $L(y)$ is valid in the range of XYZ domain and gives a first-order approximation of $L(y)$ at point y_0. Hence, the approximate mean and variance of L are obtained:

$$L(y) = 116y^{\frac{1}{3}} - 16$$

$$\cong L(y_0) + (y - y_0)L^{(1)}(y)$$

$$= 116y_0^{\frac{1}{3}} - 16 + (y - y_0)\frac{116}{3}y^{-\frac{2}{3}} \qquad (3.4)$$

Under this approximation, since $E(y-y_0) = 0$, we obtain

$$L_0 = E[L(y)] = 116y_0^{\frac{1}{3}} - 16$$

$$\sigma_L^2 = Var[L(y)] = E\left[\frac{116}{3}(y - y_0)y^{-\frac{2}{3}}\right]^2$$

$$= \left(\frac{116}{3}\right)^2 y^{-\frac{4}{3}} \cdot \sigma_y^2$$

We are now seeking a transformation $\phi(L)$ to stabilize the variance. Assuming that $\phi(L)$ has a Taylor expansion at L_0, the first-order Taylor series is used to approximate the mean and variance of $\phi(L)$, component wise.

$$\phi(L) \cong \phi(L_0) + (L - L_0)\phi^{(1)}(L_0)$$

$$\Rightarrow \quad E\phi(L) = \phi(L_0)$$

$$Var\phi(L) = E\left[\phi^{(1)}(L_0)(L - L_0)\right]^2 = \left[\phi^{(1)}(L_0)\right]^2 \sigma_L^2(L_0)$$

to stabilize the variance, which means the variance is set to be a constant

$$Var(\phi(L)) = c^2 \qquad c \text{ is a positive constant}$$

then

$$\phi^{(1)}(L_0) = \frac{c}{\sigma_L^2(L_0)}$$

from which

$$\phi(L_0) = c\int \frac{1}{\sigma_L(L_0)} dL_0$$

Substitute equation (3.4) into here, we have

$$\phi(L) = c\int \frac{1}{\sigma_L(L)}dL$$
$$= c\int \frac{3}{116} y^{\frac{2}{3}} \cdot \frac{1}{\sigma_y} dL$$

$\because$ $$L(y) = 116y^{\frac{1}{3}} - 16 \quad \Rightarrow y = \left[\frac{1}{116}(L+16)\right]^3$$

$\therefore$

$$\phi(L) = c\int \frac{3}{116}\left[\frac{1}{116}(L+16)\right]^2 \frac{1}{\sigma_y} dL$$
$$= \frac{3c}{(116)^3 \cdot \sigma_y}\int (L+16)^2 dL$$
$$= \frac{3c}{(116)^3 \cdot \sigma_y} \cdot \frac{1}{3} \cdot (L+16)^3$$
$$= \frac{c}{(116)^3 \cdot \sigma_y}(L+16)^3 \qquad (3.5)$$

- **Derivation of Transformation for *a****

For the color axis $a(x,y) = 500 \cdot [(\frac{x}{X_n})^{\frac{1}{3}} - (\frac{y}{Y_n})^{\frac{1}{3}}]$, the Taylor expansion of *a(x, y)* at point (x_0, y_0) can give the first-order approximation of *a(x, y)*.

$$a \cong a(x_0 y_0) + \frac{\partial a^{(1)}(x,y)}{\partial x}(x - x_0) + \frac{\partial a^{(1)}(x,y)}{\partial y}(y - y_0)$$

$$= 500 \cdot \left[\left(\frac{x_0}{X_n} \right)^{\frac{1}{3}} - \left(\frac{y_0}{Y_n} \right)^{\frac{1}{3}} \right] + \frac{1}{3} \cdot 500 \cdot \left(\frac{x_0}{X_n} \right)^{-\frac{2}{3}} \cdot \frac{1}{x_n} \cdot (x - x_0) - \frac{1}{3} \cdot 500 \cdot \left(\frac{y_0}{Y_n} \right)^{-\frac{2}{3}} \cdot \frac{1}{y_n} \cdot (y - y_0)$$

Under the approximation, we can obtain the approximate mean and variance of *a*.

$$a_0 = E[a(x,y)] = 500 \cdot \left[\left(\frac{x_0}{X_n} \right)^{\frac{1}{3}} - \left(\frac{y_0}{Y_n} \right)^{\frac{1}{3}} \right] \tag{3.6}$$

$$\sigma_a^2 = Var[a(x,y)] = \left(\frac{1}{3} \cdot 500 \right)^2 \cdot \left[\left(\frac{x_0}{X_n} \right)^{-\frac{2}{3}} \cdot \frac{1}{x_n} \cdot \sigma_x - \left(\frac{y_0}{Y_n} \right)^{-\frac{2}{3}} \cdot \frac{1}{y_n} \cdot \sigma_y \right]^2 \tag{3.7}$$

Assume that the transformation $\phi(a)$ we are now pursuing has Taylor expansion at point a_0, therefore the first-order expansion can give us a approximate mean and variance of $\phi(a)$, component wise.

$$\because \quad \phi(a) \cong \phi(a_0) + (a - a_0) \cdot \phi^{(1)}(a_0)$$

$$\therefore \quad E[\phi(a)] = \phi(a_0)$$

$$Var[\phi(a)] = E\left[(a - a_0) \cdot \phi^{(1)}(a_0) \right]^2$$

$$= \sigma_a^2 \left[\phi^{(1)}(a_0) \right]^2$$

To stabilize the variance, we set

$$Var\phi(a) = c^2$$

$$\Rightarrow \quad \phi(a) = c \int \frac{1}{\sigma_a} da \tag{3.8}$$

From equation (3.7), we have the variance of *a*.

Since $L(y)=116\cdot\left(\frac{y}{Y_n}\right)^{\frac{1}{3}}-16$, we can obtain

$$\left(\frac{y}{Y_n}\right)^{\frac{1}{3}}=\left[\frac{1}{116}(L+16)\right] \tag{3.9}$$

Substitute (3.9) in (3.7)

$$a(x,y)=500\left[\left(\frac{x}{X_n}\right)^{\frac{1}{3}}-\left(\frac{y}{Y_n}\right)^{\frac{1}{3}}\right]$$

$$\Rightarrow \quad a(x,y)=500\left[\left(\frac{x}{X_n}\right)^{\frac{1}{3}}-\frac{1}{116}(L+16)\right]$$

$$\Rightarrow \quad \left(\frac{x}{X_n}\right)^{\frac{1}{3}}=\frac{1}{500}a+\frac{1}{116}(L+16)$$

$$=\frac{1}{116}L+\frac{1}{500}a+\frac{16}{116} \tag{3.10}$$

Substitute equtions (3.9) and (3.10) into σ_a,

$$\sigma_a(a,L)=\frac{500}{3}\left[\frac{\sigma_x}{X_n}\left(\frac{1}{116}L+\frac{1}{500}a+\frac{16}{116}\right)^{-2}-\frac{\sigma_y}{Y_n}\left(\frac{1}{116}L+\frac{16}{116}\right)^{-2}\right] \tag{3.11}$$

$$\phi(a)=c\iint\frac{1}{\sigma_a(a,L)}dadL$$

$$=\frac{3c}{500}\cdot\iint\left[\frac{\sigma_x}{X_n}\cdot\left(\frac{1}{116}L+\frac{1}{500}a+\frac{16}{116}\right)^{-2}-\frac{\sigma_y}{Y_n}\left(\frac{1}{116}L+\frac{16}{116}\right)^{-2}\right]^{-1}dadL \tag{3.12}$$

Set $\quad m=\frac{1}{116}L+\frac{16}{116}, \qquad n=\frac{1}{500}a$

$$\Rightarrow \quad L=116\cdot\left(m-\frac{16}{116}\right), \quad a=500\cdot n$$

$$\phi(a) = 3\cdot 116\cdot c\iint\left[\frac{\sigma_x}{X_n}(m+n)^{-2} - \frac{\sigma_y}{Y_n}m^{-2}\right]^{-1} dmdn$$

$$= 3\cdot 116\cdot c\iint\left[\frac{\sigma_x Y_n m^2 - \sigma_y X_n (m+n)^2}{X_n Y_n m^2 (m+n)^2}\right]^{-1} dmdn$$

$$= 3\cdot 116\cdot c\iint\frac{X_n Y_n m^2 (m+n)^2}{\sigma_x Y_n m^2 - \sigma_y X_n (m+n)^2} dmdn$$

Set $u = m+n \quad \Rightarrow \quad n = u-m$

$$\phi(a) = 3\cdot 116\cdot c\cdot X_n\cdot Y_n\iint\frac{m^2u^2}{\sigma_x Y_n m^2 - \sigma_y X_n u^2} dmdu$$

$$= 3\cdot 116\cdot c\cdot\frac{X_n Y_n}{\sigma_x Y_n}\iint\frac{\sigma_x Y_n m^2u^2 - \sigma_y X_n m^4 + \sigma_y X_n m^4}{\sigma_x Y_n m^2 - \sigma_y X_n u^2} dmdu$$

$$= 3\cdot 116\cdot c\cdot\frac{X_n}{\sigma_x}\iint\left[m^2 + \frac{\sigma_y X_n m^4}{\sigma_x Y_n m^2 - \sigma_y X_n u^2}\right] dmdu$$

$$= 3\cdot 116\cdot c\cdot\frac{X_n}{\sigma_x}\int m^2\int\left[1 - \frac{\sigma_y X_n m^2}{\sigma_y X_n u^2 - \sigma_x Y_n m^2}\right] dudm$$

$$= 3\cdot 116\cdot c\cdot\frac{X_n}{\sigma_x}\int m^2\left[\int 1du - \sigma_y X_n m^2\underbrace{\int\frac{1}{\sigma_y X_n u^2 - \sigma_x Y_n m^2} du}_{(3.13)}\right] dm$$

According to the integration formula $\int\frac{du}{u^2-a^2} = \frac{1}{2a}\ln\frac{u-a}{u+a} + C$, the equation (3.13) can be rewritten as,

$$\int\frac{1}{\sigma_y X_n u^2 - \sigma_x Y_n m^2} du = \frac{1}{2\sqrt{\sigma_x\sigma_y X_n Y_n}\cdot m}\ln\frac{\sqrt{\sigma_y X_n}\cdot u - \sqrt{\sigma_x Y_n}\cdot m}{\sqrt{\sigma_y X_n}\cdot u + \sqrt{\sigma_x Y_n}\cdot m}$$

$$\therefore \quad \phi(a) = 3\cdot 116\cdot c\cdot \frac{X_n}{\sigma_x}\int\left(m^2 u - m^3 \frac{\sqrt{\sigma_y X_n}}{2\sqrt{\sigma_x Y_n}} \ln \frac{\sqrt{\sigma_y X_n}\cdot u - \sqrt{\sigma_x Y_n}\cdot m}{\sqrt{\sigma_y X_n}\cdot u + \sqrt{\sigma_x Y_n}\cdot m}\right) dm$$

$$= 3\cdot 116\cdot c\cdot \frac{X_n}{\sigma_x}\left[\frac{1}{3}m^3 u - \frac{\sqrt{\sigma_y X_n}}{2\sqrt{\sigma_x Y_n}}\int m^3 \left[\begin{array}{l} \ln\left(\sqrt{\sigma_y X_n}\cdot u - \sqrt{\sigma_x Y_n}\cdot m\right) \\ -\ln\left(\sqrt{\sigma_y X_n}\cdot u + \sqrt{\sigma_x Y_n}\cdot m\right) \end{array} \right] dm \right] \qquad (3.14)$$

Set $d_0 = \sqrt{\sigma_y X_n}$, $d_1 = \sqrt{\sigma_x Y_n}$, and according to integration formula

$$\int x^n \ln(a+bx)dx = \frac{1}{4}\left(x^4 - \frac{a^4}{b^4}\right)\ln(a+bx) - \frac{1}{4}\left(\frac{x^4}{4} - \frac{ax^3}{3b} + \frac{a^2x^2}{2b^2} - \frac{a^3x}{b^3}\right),$$

we have,

$$\int m^3 \ln(d_0 u - d_1 m)dm$$
$$= \frac{1}{4}\left(m^4 - \frac{{d_0}^4}{{d_1}^4}u^4\right)\ln(d_0 u - d_1 m) - \frac{1}{4}\left(\frac{m^4}{4} + \frac{d_0 u m^3}{3d_1} + \frac{{d_0}^2 u^2 m^2}{2{d_1}^2} + \frac{{d_0}^3 u^3 m}{{d_1}^3}\right)$$

$$\int m^3 \ln(d_0 u + d_1 m)dm$$
$$= \frac{1}{4}\left(m^4 - \frac{{d_0}^4}{{d_1}^4}u^4\right)\ln(d_0 u + d_1 m) - \frac{1}{4}\left(\frac{m^4}{4} - \frac{d_0 u m^3}{3d_1} + \frac{{d_0}^2 u^2 m^2}{2{d_1}^2} - \frac{{d_0}^3 u^3 m}{{d_1}^3}\right)$$

$\therefore$

$$\phi(a) = 3\cdot 116\cdot c\cdot \frac{X_n}{\sigma_x}\left\{ \frac{1}{3}m^3 u - \frac{d_0}{2d_1}\cdot\left[\frac{1}{4}\left(m^4 - \frac{{d_0}^4}{{d_1}^4}u^4\right)\ln\frac{d_0 u - d_1 m}{d_0 u + d_1 m} - \frac{1}{2}\left(\frac{d_0 u m^3}{3d_0} + \frac{{d_0}^3 u^3 m}{{d_1}^3}\right)\right]\right\} \qquad (3.15)$$

where

$u = m + n, \qquad m = \frac{1}{116}L + \frac{16}{116}$

$d_0 = \sqrt{\sigma_y X_n}, d_1 = \sqrt{\sigma_x Y_n}$ are constants.

This transformation is monotonously increased in the area that covers the range of the color space, it's suitable to be used to stabilize the signal dependent variance caused by

the nonlinear transformation from XYZ domain to $L^*a^*b^*$ domain. However due to its computation complexity, it's difficult to derive the corresponding inverse function so that a linear approximation of this transformation is used instead. By taking a Taylor expansion at point a=0, Equation (3.15) can be simplified as,

$$\phi(a) \approx \phi(0) + \phi'(0) \cdot a$$

$$= \frac{3 \cdot 116 \cdot c \cdot X_n}{\sigma_x} \left[\frac{m^4}{3} - \frac{d_0}{2d_1} \cdot \frac{1}{4} \left(m^4 - \frac{d_0^4}{d_1^4} m^4 \right) \ln \frac{(d_0 - d_1)}{(d_0 + d_1)} - \frac{d_0}{4d_1} \left(\frac{d_0 m^4}{3d_1} + \frac{d_0^3 m^4}{d_1^3} \right) \right] +$$

$$\frac{3 \cdot 116 \cdot c \cdot X_n}{\sigma_x} \left[\begin{array}{l} \frac{m^3}{1500} - \frac{d_0^5 m^3}{1000 d_1^5} \ln \frac{d_0 - d_1}{d_0 + d_1} - \frac{1}{2000} \left(1 - \frac{d_0^4}{d_1^4} \right) \frac{d_0^2}{d_0^2 - d_1^2} m^3 \\ - \frac{d_0^2}{2000 d_1^2} \left(\frac{1}{3} + \frac{3 d_0^2}{d_1^2} \right) m^3 \end{array} \right] \cdot a$$

$\phi(a)$ is approximated as

$$\phi(a) = k_1 \left(\frac{1}{116} L + \frac{16}{116} \right)^3 a + k_2 \left(\frac{1}{116} L + \frac{16}{116} \right)^4 \tag{3.16}$$

where

$$k_1 = \frac{3 \cdot 116 \cdot c \cdot X_n}{\sigma_x} \left[\begin{array}{l} \frac{1}{1500} - \frac{d_0^5}{1000 d_1^5} \ln \frac{d_0 - d_1}{d_0 + d_1} + \frac{d_0^2 (d_0^2 + d_1^2)}{2000 d_1^4} \\ - \frac{d_0^2}{2000 d_1^2} \left(\frac{1}{3} + \frac{3 d_0^2}{d_1^2} \right) \end{array} \right]$$

$$k_2 = \frac{3 \cdot 116 \cdot c \cdot X_n}{\sigma_x} \left[\frac{1}{3} - \frac{d_0}{8d_1} \left(1 - \frac{d_0^4}{d_1^4} \right) \ln \frac{(d_0 - d_1)}{(d_0 + d_1)} - \frac{d_0^2}{4d_1^2} \left(\frac{1}{3} + \frac{d_0^2}{d_1^2} \right) \right]$$

- **Derivation of Transformation for b^***

The derivation procedure of $\phi(b)$ is similar to $\phi(a)$. The Taylor expansion of $b(y,z) = 200 \cdot [(\frac{y}{Y_n})^{\frac{1}{3}} - (\frac{z}{Z_n})^{\frac{1}{3}}]$ at point (y_0, z_0) can give us the first-order approximation of $b(y, z)$, where y_0, z_0 are the mean of y, z respectively.

$$b(y,z) \cong b(y_0,z_0) + \frac{\partial b^{(1)}(y,z)}{\partial y}(y-y_0) + \frac{\partial b^{(1)}(y,z)}{\partial z}(z-z_0)$$

$$= 200 \cdot \left[\left(\frac{y_0}{Y_n}\right)^{\frac{1}{3}} - \left(\frac{z_0}{Z_n}\right)^{\frac{1}{3}} \right] + \frac{1}{3} \cdot 200 \cdot \left(\frac{y_0}{Y_n}\right)^{-\frac{2}{3}} \cdot \frac{1}{Y_n} \cdot (y-y_0) - \frac{1}{3} \cdot 200 \cdot \left(\frac{z_0}{Z_n}\right)^{-\frac{2}{3}} \cdot \frac{1}{Z_n} \cdot (z-z_0)$$

Under this approximation, we have

$$b_0 = E[b(y,z)] = 200 \cdot \left[\left(\frac{y_0}{Y_n}\right)^{\frac{1}{3}} - \left(\frac{z_0}{Z_n}\right)^{\frac{1}{3}} \right] \tag{3.17}$$

$$\sigma_b^2 = Var[b(y,z)] = \left(\frac{1}{3} \cdot 200\right)^2 \cdot \left[\left(\frac{y_0}{Y_n}\right)^{-\frac{2}{3}} \cdot \frac{1}{Y_n} \cdot \sigma_y - \left(\frac{z_0}{Z_n}\right)^{-\frac{2}{3}} \cdot \frac{1}{Z_n} \cdot \sigma_z \right]^2 \tag{3.18}$$

Assume that the transformation $\phi(b)$ we are now pursuing has Taylor expansion at point b_0, therefore the first-order expansion can give us a approximate mean and variance of $\phi(b)$, component wise.

$\because$ $\quad \phi(b) \cong \phi(b_0) + (b-b_0) \cdot \phi^{(1)}(b_0)$

$\therefore$ $\quad E\phi(b) = \phi(b_0)$

$$Var\phi(b) = E\left[(b-b_0) \cdot \phi^{(1)}(b_0)\right]^2$$

$$= \sigma_b^2 \left[\phi^{(1)}(b_0)\right]^2$$

To stabilize the variance, we set

$$Var\phi(b) = c^2$$

$$\Rightarrow \qquad \phi(b) = c\int \frac{1}{\sigma_b} db \tag{3.19}$$

From equation (3.18), we already have the variance of b.

Since $L(y) = 116 \cdot \left(\frac{y}{Y_n}\right)^{\frac{1}{3}} - 16$, we can obtain

$$\left(\frac{y}{Y_n}\right)^{\frac{1}{3}} = \left[\frac{1}{116}(L+16)\right] \tag{3.20}$$

Therefore,

$$b(y,z) = 200\left[\left(\frac{y}{Y_n}\right)^{\frac{1}{3}} - \left(\frac{z}{Z_n}\right)^{\frac{1}{3}}\right]$$

$$\Rightarrow \qquad b(y,z) = 200\left[\frac{1}{116}(L+16) - \left(\frac{z}{Z_n}\right)^{\frac{1}{3}}\right]$$

$$\Rightarrow \qquad \left(\frac{z}{Z_n}\right)^{\frac{1}{3}} = \frac{1}{116}(L+16) - \frac{1}{200}b$$

$$= \frac{1}{116}L - \frac{1}{200}b + \frac{16}{116} \tag{3.21}$$

Substitute equations (3.20) and (3.21) into σ_b,

$$\sigma_b(b,L) = \frac{200}{3}\left[\frac{\sigma_y}{Y_n}\left(\frac{1}{116}L + \frac{16}{116}\right)^{-2} - \frac{\sigma_z}{Z_n}\left(\frac{1}{116}L - \frac{1}{200}b + \frac{16}{116}\right)^{-2}\right] \tag{3.22}$$

and substitute (3.22) into (3.19), then

$$\phi(b) = c\iint \frac{1}{\sigma_b(b,L)}\,dbdL$$

$$= \frac{3c}{200}\cdot\iint\left[\frac{\sigma_y}{Y_n}\cdot\left(\frac{1}{116}L+\frac{16}{116}\right)^{-2} - \frac{\sigma_z}{Z_n}\left(\frac{1}{116}L-\frac{1}{200}b+\frac{16}{116}\right)^{-2}\right]^{-1} dbdL \qquad (3.23)$$

Set $\quad m = \frac{1}{116}L+\frac{16}{116}, \qquad n = \frac{1}{200}b$

$\Rightarrow \quad L = 116\cdot\left(m-\frac{16}{116}\right), \quad b = 200\cdot n$

and we have,

$$\phi(b) = 3\cdot 116\cdot c\iint\left[\frac{\sigma_y}{Y_n}m^{-2} - \frac{\sigma_z}{Z_n}(m-n)^{-2}\right]^{-1} dmdn$$

$$= 3\cdot 116\cdot c\iint\left[\frac{\sigma_y Z_n(m-n)^2 - \sigma_z Y_n m^2}{Y_n Z_n m^2(m-n)^2}\right]^{-1} dmdn$$

$$= 3\cdot 116\cdot c\iint\frac{Y_n Z_n m^2(m-n)^2}{\sigma_y Z_n(m-n)^2 - \sigma_z Y_n m^2}\,dmdn$$

Set $\quad u = m-n \quad \Rightarrow \quad n = m-u$

$$\phi(b) = -3\cdot 116\cdot c\cdot Y_n\cdot Z_n \iint \frac{m^2u^2}{\sigma_y Z_n u^2 - \sigma_z Y_n m^2}\,dmdu$$

$$= -3\cdot 116\cdot c\cdot \frac{Y_n Z_n}{\sigma_y Z_n} \iint \frac{\sigma_y Z_n m^2u^2 - \sigma_z Y_n m^4 + \sigma_z Y_n m^4}{\sigma_y Z_n u^2 - \sigma_z Y_n m^2}\,dmdu$$

$$= -3\cdot 116\cdot c\cdot \frac{Y_n}{\sigma_y} \iint \left[m^2 + \frac{\sigma_z Y_n m^4}{\sigma_y Z_n u^2 - \sigma_z Y_n m^2} \right] dmdu$$

$$= -3\cdot 116\cdot c\cdot \frac{Y_n}{\sigma_y} \int m^2 \int \left[1 + \frac{\sigma_z Y_n m^2}{\sigma_y Z_n u^2 - \sigma_z Y_n m^2} \right] dudm$$

$$= -3\cdot 116\cdot c\cdot \frac{Y_n}{\sigma_y} \int m^2 \left[\int 1du + \sigma_z Y_n m^2 \underbrace{\int \frac{1}{\sigma_y Z_n u^2 - \sigma_z Y_n m^2}\,du}_{(3.24)} \right] dm$$

According to the integration formula $\int \frac{du}{u^2 - a^2} = \frac{1}{2a}\ln\frac{u-a}{u+a} + C$, the equation (3.24) is rewritten as,

$$\int \frac{1}{\sigma_y Z_n u^2 - \sigma_z Y_n m^2}\,du = \frac{1}{2\sqrt{\sigma_y \sigma_z Y_n Z_n}\cdot m} \ln \frac{\sqrt{\sigma_y Z_n}\cdot u - \sqrt{\sigma_z Y_n}\cdot m}{\sqrt{\sigma_y Z_n}\cdot u + \sqrt{\sigma_z Y_n}\cdot m}$$

$$\therefore \quad \phi(b) = -3\cdot 116\cdot c\cdot \frac{Y_n}{\sigma_y} \int \left(m^2u + m^3 \frac{\sqrt{\sigma_z Y_n}}{2\sqrt{\sigma_y Z_n}} \ln \frac{\sqrt{\sigma_y Z_n}\cdot u - \sqrt{\sigma_z Y_n}\cdot m}{\sqrt{\sigma_y Z_n}\cdot u + \sqrt{\sigma_z Y_n}\cdot m} \right) dm$$

$$= -3\cdot 116\cdot c\cdot \frac{Y_n}{\sigma_y} \left[\frac{1}{3}m^3u + \frac{\sqrt{\sigma_z Y_n}}{2\sqrt{\sigma_y Z_n}} \int m^3 \left[\begin{array}{l} \ln\left(\sqrt{\sigma_y Z_n}\cdot u - \sqrt{\sigma_z Y_n}\cdot m\right) - \\ \ln\left(\sqrt{\sigma_y Z_n}\cdot u + \sqrt{\sigma_z Y_n}\cdot m\right) \end{array} \right] dm \right] \qquad (3.25)$$

Set $d_2 = \sqrt{\sigma_y Z_n}$, $d_3 = \sqrt{\sigma_z Y_n}$, and we have,

$$\int m^3 \ln(d_2 u - d_3 m) dm$$

$$= \frac{1}{4}\left(m^4 - \frac{{d_2}^4}{{d_3}^4} u^4\right) \ln(d_2 u - d_3 m) - \frac{1}{4}\left(\frac{m^4}{4} + \frac{d_2 u m^3}{3 d_3} + \frac{{d_2}^2 u^2 m^2}{2 {d_3}^2} + \frac{{d_2}^3 u^3 m}{{d_3}^3}\right)$$

and

$$\int m^3 \ln(d_2 u + d_3 m) dm$$

$$= \frac{1}{4}\left(m^4 - \frac{{d_2}^4}{{d_3}^4} u^4\right) \ln(d_2 u - d_3 m) - \frac{1}{4}\left(\frac{m^4}{4} - \frac{d_2 u m^3}{3 d_3} + \frac{{d_2}^2 u^2 m^2}{2 {d_3}^2} - \frac{{d_2}^3 u^3 m}{{d_3}^3}\right)$$

$\therefore$

$$\phi(b) = -3 \cdot 116 \cdot c \cdot \frac{Y_n}{\sigma_y} \left\{ \frac{1}{3} m^3 u + \frac{d_3}{2 d_2} \cdot \left[\begin{array}{l} \frac{1}{4}\left(m^4 - \frac{{d_2}^4}{{d_3}^4} u^4\right) \ln \frac{d_2 u - d_3 m}{d_2 u + d_3 m} - \\ \frac{1}{2}\left(\frac{d_2 u m^3}{3 d_3} + \frac{{d_2}^3 u^3 m}{{d_3}^3}\right) \end{array} \right] \right\} \tag{3.26}$$

Where

$$u = m - n, \qquad m = \frac{1}{116} L + \frac{16}{116}, \qquad n = \frac{1}{200} b,$$

$d_2 = \sqrt{\sigma_z Y_n}$ and $d_3 = \sqrt{\sigma_y Z_n}$ are constants.

Similarly to transformation $\phi(a)$, a first order Taylor series expansion is used to approximate $\phi(b)$ at point $b=0$ in a linear form.

$$\phi(b) \approx \phi(0) + \phi'(0) * b$$

$$= -\frac{3 \cdot 116 \cdot c \cdot Y_n}{\sigma_y} \left[\frac{m^4}{3} + \frac{d_3}{2 d_2} \cdot \frac{1}{4}\left(m^4 - \frac{{d_2}^4}{{d_3}^4} m^4\right) \ln \frac{(d_2 - d_3)}{(d_2 + d_3)} - \frac{d_3}{4 d_2}\left(\frac{d_2 m^4}{3 d_3} + \frac{{d_2}^3 m^4}{{d_3}^3}\right) \right] +$$

$$\frac{3 \cdot 116 \cdot c \cdot Y_n}{\sigma_y} \left[\frac{m^3}{600} - \frac{{d_2}^3 m^3}{400 {d_3}^3} \ln \frac{d_2 - d_3}{d_2 + d_3} - \frac{1}{800}\left(1 - \frac{{d_2}^4}{{d_3}^4}\right) \frac{d_2 d_3}{\left({d_2}^2 - {d_3}^2\right)} m^3 - \frac{1}{800}\left(\frac{1}{3} + \frac{3 {d_2}^2}{{d_3}^2}\right) m^3 \right] \cdot b$$

Therefore, $\phi(b)$ is approximated as

$$\phi(b) = k_3\left(\frac{1}{116}L + \frac{16}{116}\right)^3 b + k_4\left(\frac{1}{116}L + \frac{16}{116}\right)^4 \tag{3.27}$$

where

$$k_3 = \frac{3\cdot 116\cdot c\cdot Y_n}{\sigma_y}\left[\frac{1}{600} - \frac{{d_2}^3}{400{d_3}^3}\ln\frac{d_2 - d_3}{d_2 + d_3} + \frac{d_2\left({d_2}^2 + {d_3}^2\right)}{800{d_3}^3} - \frac{1}{800}\left(\frac{1}{3} + \frac{3{d_2}^2}{{d_3}^2}\right)\right]$$

$$k_4 = -\frac{3\cdot 116\cdot c\cdot Y_n}{\sigma_y}\left[\frac{1}{3} + \frac{d_2}{2d_3}\left(1 - \frac{{d_2}^4}{{d_3}^4}\right)\ln\frac{(d_2 - d_3)}{(d_2 + d_3)} - \frac{1}{4}\left(\frac{1}{3} + \frac{{d_2}^2}{{d_3}^2}\right)\right]$$

Chapter 4 Simulation Results

In this chapter, evaluations are performed quantitatively to demonstrate the effectiveness of the switch filters, and a comparison is made between the switch filters and the Sigma filter to measure the performance of the switch filter scheme.

Three factors are critical when evaluating the performance of noise removal filters in processing color images. The first one is the ability of noise reduction, another is the ability to preserving edges and details; the last one is to preserve the chromatic information of the image as much as possible. The first requirement and the latter two are usually believed as a trade-off that noise is removed with the expense of smoothing the image details and changing the color appearance. Therefore an overall evaluation of all three aspects can give us a better understanding of the quality of this noise-removing switch scheme.

4.1 Measures of image quality

To measure the efficiency of any image filtering method, the easiest and simplest approach is the subjective comparison of the filtered image and the uncorrupted original image. However, objective evaluations are widely used because visual observation cannot provide a straightforward quantity to determine the quality of the filters.

Two objective measures are used for the purpose of analysis. The normalized mean square error (NMSE) is chosen since it's the most widely used measurement, which is defined in the RGB color space as:

$$NMSE = E\left(\frac{\sum_{i=0}^{n}\sum_{j=0}^{m}\left\|f(i,j)-\hat{f}(i,j)\right\|^2}{\sum_{i=0}^{n}\sum_{j=0}^{m}\left\|\hat{f}(i,j)\right\|^2}\right) \tag{4.1}$$

where n, m are the image dimensions, $f(i, j)$ and $\hat{f}(i,j)$ denote the original image vector and the estimation at pixel (i, j), respectively.

The perceptual closeness is another consideration when filtering color image. The RGB color space is not appropriate to quantify the perception of color. Thus, color difference between the filtered image and the original one is calculated in a perceptually uniform color spaces, CIE $L^*a^*b^*$ color space, which is related to the human vision characteristics. The normalized color distance (NCD) is defined as:

$$NCD = E\left(\frac{\sum_{i=1}^{n}\sum_{j=1}^{m}\Delta E}{\sum_{i=1}^{n}\sum_{j=1}^{m}E^*}\right) \tag{4.2}$$

$$\Delta E = [(\Delta L)^2 + (\Delta a)^2 + (\Delta b)^2]^{\frac{1}{2}}$$

$$E^* = [(L^*)^2 + (a^*)^2 + (b^*)^2]^{\frac{1}{2}}$$

where ΔE is the perceptual color error and E^* is the magnitude of the uncorrupted original color image pixel in the $L^*a^*b^*$ space.

4.2 Quantitatively Evaluation

4.2.1 Methodology

The first step of the evaluation is to set up a methodology to detect the spatial activity of the image. Spatial activity is defined as the ratio of the change of color,

including both chromaticity and lightness, from one pixel to its neighbouring pixels. Based on the spatial information, the image can be partitioned into different segments according to the levels of spatial activity. What we interest here are two types of segments – the segments with edges and the flat segments. An ideal image is assumed to be piecewise constant in the flat segments and a simple ramp for edge segments.

For a digital function, the derivatives are defined in terms of differences. It's well known that the greyscale intensity change and orientation information in an image can be detected using the first derivative operators [19]. Though the forms of these operators are varied, they must meet the following requirements.

1) They must be zero in flat segments (indicating no change of greyscale values);
2) They must be nonzero at the onset of a greyscale step or ramp;
3) They must be nonzero along ramps.

Prewitt operator is one of the most popular filters for edge detection. It's a 3×3 row and column impulse response array as

$$\Delta H = \frac{1}{3}\begin{bmatrix} -1 & 0 & 1 \\ -1 & 0 & 1 \\ -1 & 0 & 1 \end{bmatrix}$$

to detect edges in the horizontal direction with $\theta = 0°$, and,

$$\Delta V = \frac{1}{3}\begin{bmatrix} -1 & -1 & -1 \\ 0 & 0 & 0 \\ 1 & 1 & 1 \end{bmatrix}$$

to detect edges in the vertical direction with $\theta = 270°$.

The edge detection in colour image shares the similar concepts with those of the greyscale image. For an operating window size 3×3, the directional operators from [20] can be presented as following:

$$\Delta H = \frac{1}{3}\begin{bmatrix} -I & 0 & I \end{bmatrix} \tag{4.3}$$

for the horizontal direction and

$$\Delta V = \frac{1}{3}\begin{bmatrix} -I \\ 0 \\ I \end{bmatrix} \tag{4.4}$$

for the vertical direction, where I is a 3×3 matrix with all ones and 0 is a 3×3 matrix with all zeros in the third dimension. The directional operators can be considered as the extension of the Prewitt operator to the color image because the operators estimate the colour gradient of the three-dimensional images in a similar approach as Prewitt operator runs in greyscale image to detect the discontinuities.

With the output $S(\bar{x})$ of the directional operators applied to a given image f, the image can be divided into several subsets R_i in terms of spatial activity based on the partition threshold t_i. The subsets satisfy the condition that $\cup_{all\, i} R_i = f$ and $R_i \cap R_j = \phi$ if $i \neq j$.

In the evaluation, four masks of the directional operators were used to determine the spatial altering of the test image. In addition to the two masks listed above, which used to detect edges of 0° and 270° degree, another two vector gradient operators are also used to detect edges along the direction of 90° and 180° degree.

$$\Delta V^{-} = \frac{1}{3}\begin{bmatrix} I \\ 0 \\ -I \end{bmatrix} \qquad \Delta H^{-} = \frac{1}{3}[I \quad 0 \quad -I]$$

Therefore the output $S(\bar{x})$ as the combination of four directional operators is

$$S(\bar{x}) = |f_{\bar{x}} * \Delta H| + |f_{\bar{x}} * \Delta H^{-}| + |f_{\bar{x}} * \Delta V| + |f_{\bar{x}} * \Delta V^{-}| \tag{4.6}$$

If $t_i < S(\bar{x}) < t_{i+1}$, the pixel $\bar{x}$ is assumed to be in region R_i. By this approach, all pixels in the image are classified into appropriate subset $R_i, i = 1,2,3...,k$. With the subsets information, the performance of the noise removal filters can be assessed in different areas with different levels of spatial activity.

4.2.2 Evaluation Results of Artificial Image

A test image is generated specifically to evaluate the colour and edge preservation effect of the filters while removing the noise.

The artificial image is constructed in $L^*a^*b^*$ domain with dimensions 120*120 pixels. In the center of the image is a circle as the foreground with radius 25 pixels and the background uses a different color. The central circle and the background are both filled with solid colors. While between them, the ramp edge is established by color transition from the foreground colour to that of the background.

The image has a constant hue, which means that there's no lightness altering along the L* coordinates, but a color transformation in the edge segment along the a^* axis from green as the foreground to magenta as the background.

The spatial activity of the test image can be identified by the approach discussed in previous session. The output results of the directional operators divided the image into two

disjoint partitions: the flat area and the area with ramp edges. Flat area means that no color altering is detected and the output of the directional operators is zero (i.e. the area inside the circle and the solid background). On the other hand, when the output of the directional operators is larger than zero, it indicates that there is color altering between the given pixel and its neighbourhood, this pixel is classified to the ramp edge area. In this particular case, obviously the transition ramp between circle and background is defined as area with edges.

Three types of noise models given by Equation (2.1) (2.2) and (2.4) are applied to the test image separately to simulate the degradations, as listed in Table 4.1. 50 corrupted images are generated independently for each type in the simulation. NMSE & NCD are calculated as the average filtered output of these 50 images processed. The original image and the noise corrupted sample are shown in Fig. 4.1 – 4.4.

Number	Noise Model
1	Gaussian noise ($\sigma = 30$)
2	Impulsive noise (10% and $p_1 = p_2 = p_3 = 0.25$, $p_7 = 0.25$)
3	Gaussian noise ($\sigma = 30$), Impulsive noise (10% and $p_1 = p_2 = p_3 = 0.25$)

Table 4.1 Noise Distributions

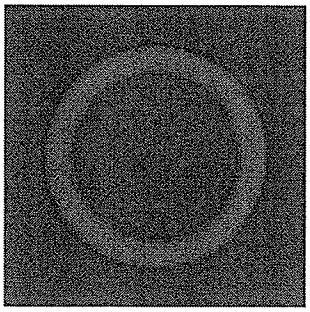

Figure 4-1Original Test Image

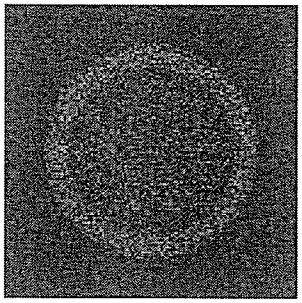

Figure 4-2 Image Corrupted by Gaussian noise

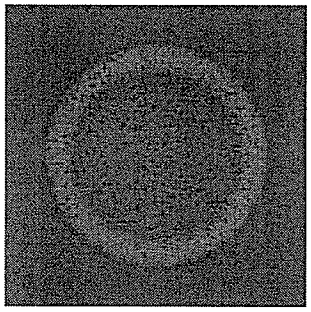

Figure 4-3 Image corrupted by impulsive noise

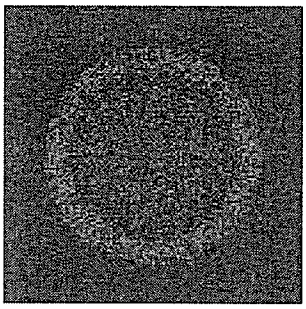

Figure 4-4 Image corrupted by mixed noise

- Effect of threshold T

First, the effects of threshold T are studied on the performance of all three types of noise models. Both the mean switch filter and the median switch filter are operated on a filtering window, whose size is 5*5. The output of these two switch filters are demonstrated in Fig. 4-5 in terms of NMSE with respect to T value altered in the range [0, 100]. Both filters give excellent results in the case of impulsive noise. A minimum of NMSE is achieved at T=10 for both filters. In both cases of Gaussian noise and mixed noise, the mean switch filter as expected reveals a better result than the median switch filter, however, NMSE of the mean switch filter grow gradually as T increases and no obvious

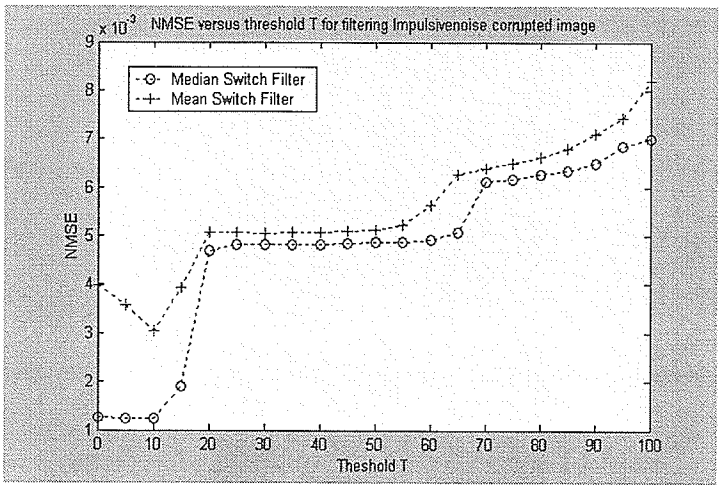

(a)

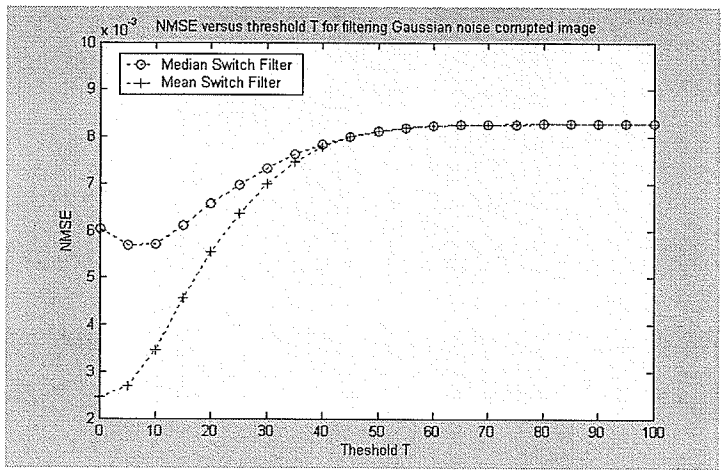

(b)

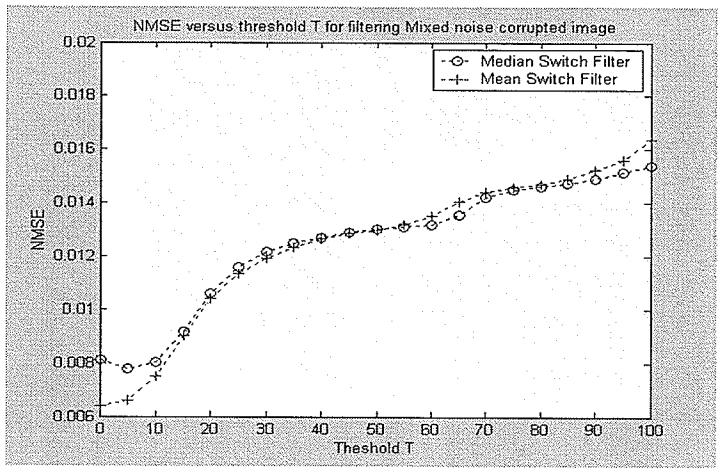

(c)

Figure 4-5 NMSE as a function of parameter k1, k3 (a) in impulsive noise case, (b) in Gaussian noise case and (c) in mixed noise case

minimum is depicted in Fig. 4-5 (b) and (c).

- Evaluations based on the spatial activity of the image

The second experiment with artificial images corrupted by different amounts of noises focuses on the filter's ability to preserve edges and color consistency. By spatial activity detecting approach discussed in preceding session 4.2.1, the test image is divided into homogenous area and ramp area. Two measurements, NMSE (normalized Mean Square error) and NCD (Normalized Color Difference), are used to objectively measure the efficiency of the proposed switch filters and compare with the result of the Sigma filter.

In the case of impulsive noise corruption, the switch scheme as expected gives excellent results both in homogenous area and at the ramp (See Fig. 4-6 (a), (b), (c) and (d)). Even the mean based switch filter can remove most of the noises, especially in terms of NCD. This observation proves that a perceptually uniform color space contributes the preservation of desired color to the switch scheme. Overall, the outcome of the switch filters is much better than the Sigma filter, as both efficient smoothing in the homogeneous region and edge preservation at the ramp edge are achieved.

In the case of Gaussian noise, the mean switch filter's performance is close to the Sigma filter's in terms of NMSE. In the ramp edge area (Fig. 4-7(a)), the Sigma filter works slightly better than the mean switch filter when noise intensities are low, but when the noise amounts increase, the mean switch filter outperforms the Sigma filter. In the flat area (Fig. 4-7(b)), due to the nature of the mean filter, the mean switch filter gives the best output. When NCD is considered, the Sigma filter and the mean switch filter give pretty

much the same result for the ramp while the mean switch filter works best for flat area (Fig. 4-7(c) and (d)).

Concluded from above observations, the switch filters work best for the impulsive noise corrupted image. However, because of the classic mean filter's ability to smooth Gaussian noise, the mean based switch filter has a nice performance of handling Gaussian noise corrupted image and preserving both necessary edge details and color information.

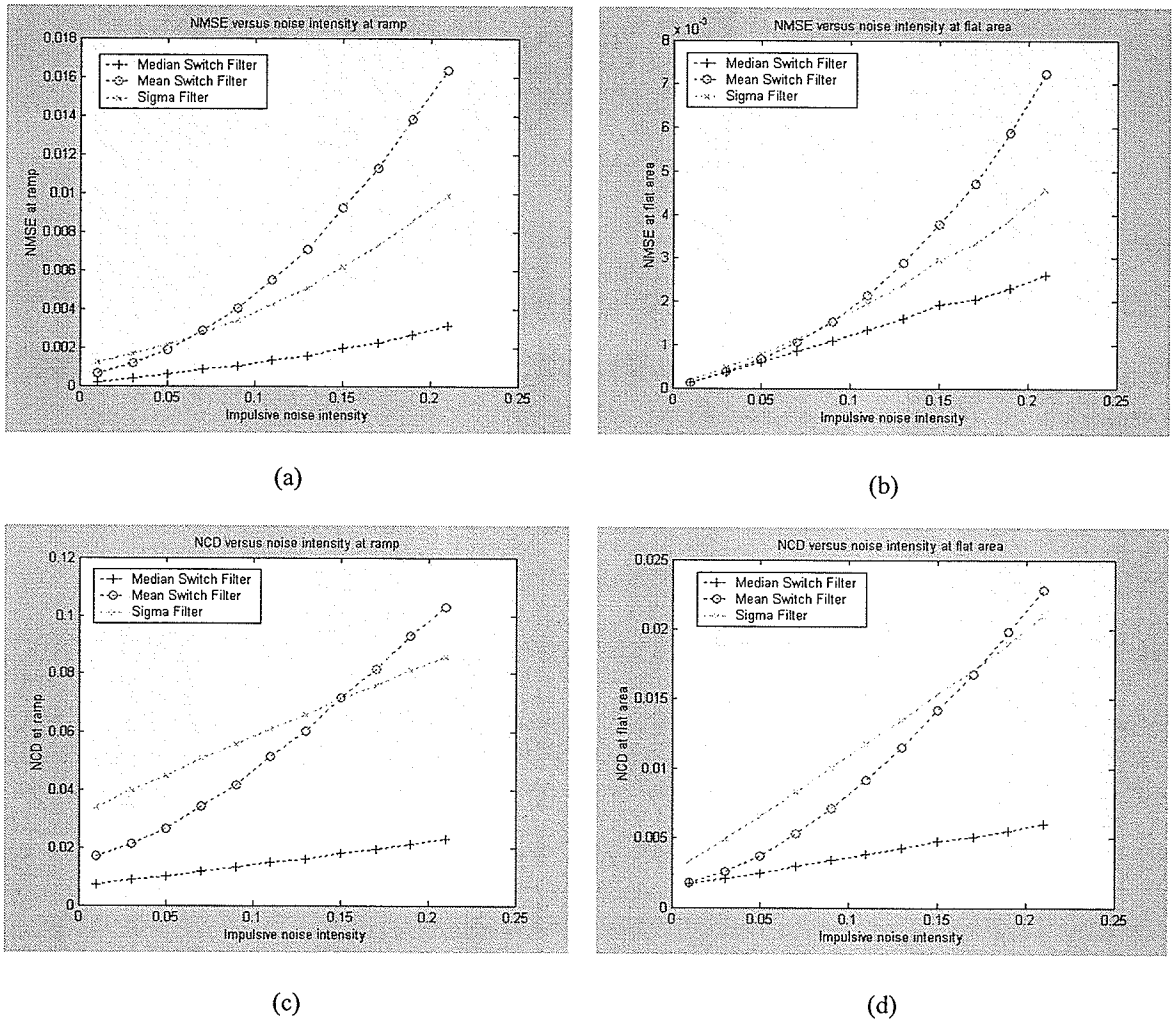

Figure 4-6 Comparison of the efficiency of the switch filters with Sigma filter for different amounts of impulsive noise intensities, in terms of (a) NMSE in ramp edge area, (b) NMSE in homogenous area, and (c) NCD in ramp area, (d) NCD in homogenous area

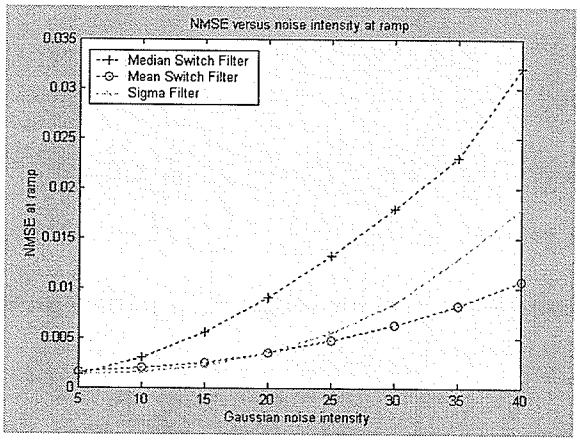

(a)

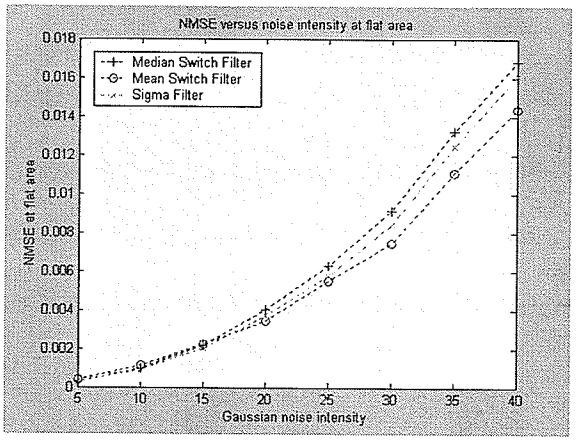

(b)

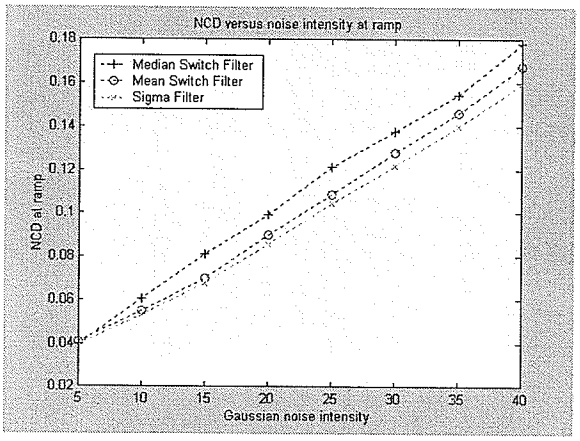

(c)

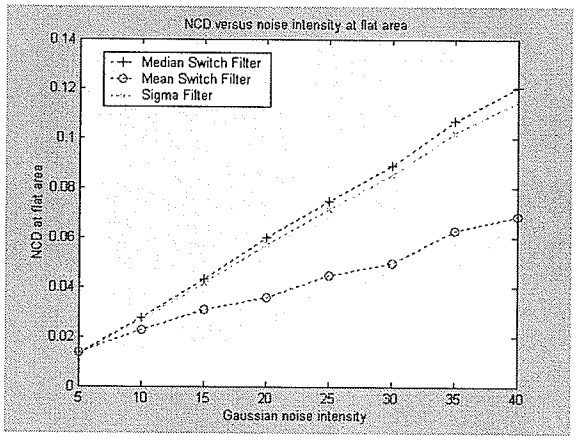

(d)

Figure 4-7 Comparison of the efficiency of the switch filters with Sigma filter for different amounts of Gaussian noise intensities, in terms of (a) NMSE in ramp edge area, (b) NMSE in homogenous area, and (c) NCD in ramp area, (d) NCD in homogenous area

4.2.3 Evaluation Results of Natural Color Image

Natural color image is also processed to test the proposed filters' behaviour. The image "building" is corrupted by the noise models listed in Table 4-1, respectively. We use

mean based switch filter, median based switch filter, and Sigma filter to remove the noises from the image. All of the filters are performed with window size 5*5. Both NMSE and NCD are the objective measures used to evaluate the efficiency of these noise removal techniques.

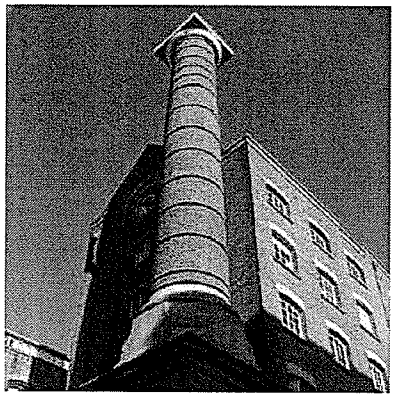

Figure 4-8 Natural Test Image

Filter	NMSE	NCD
Median Switch Filter	0.005458	0.025967
Mean Switch Filter	0.005027	0.031501
Sigma Filter	0.006375	0.088843

Table 4.2 Comparison of the efficiency of the filters, using the Building image corrupted by Impulsive noise of (p=0.1, p_1=p_2=p_3=0.25)

Filter	NMSE	NCD
Median Switch Filter	0.038563	0.197186
Mean Switch Filter	0.022144	0.101926
Sigma Filter	0.014643	0.095339

Table 4.3 Comparison of the efficiency of the filters, using the Building image corrupted by Gaussian noise of σ=30

Filter	NMSE	NCD
Median Switch Filter	0.044354	0.193810
Mean Switch Filter	0.029803	0.118882
Sigma Filter	0.012954	0.092553

Table 4.4 Comparison of the efficiency of the filters, using the Building image corrupted by mixed impulsive and Gaussian noise

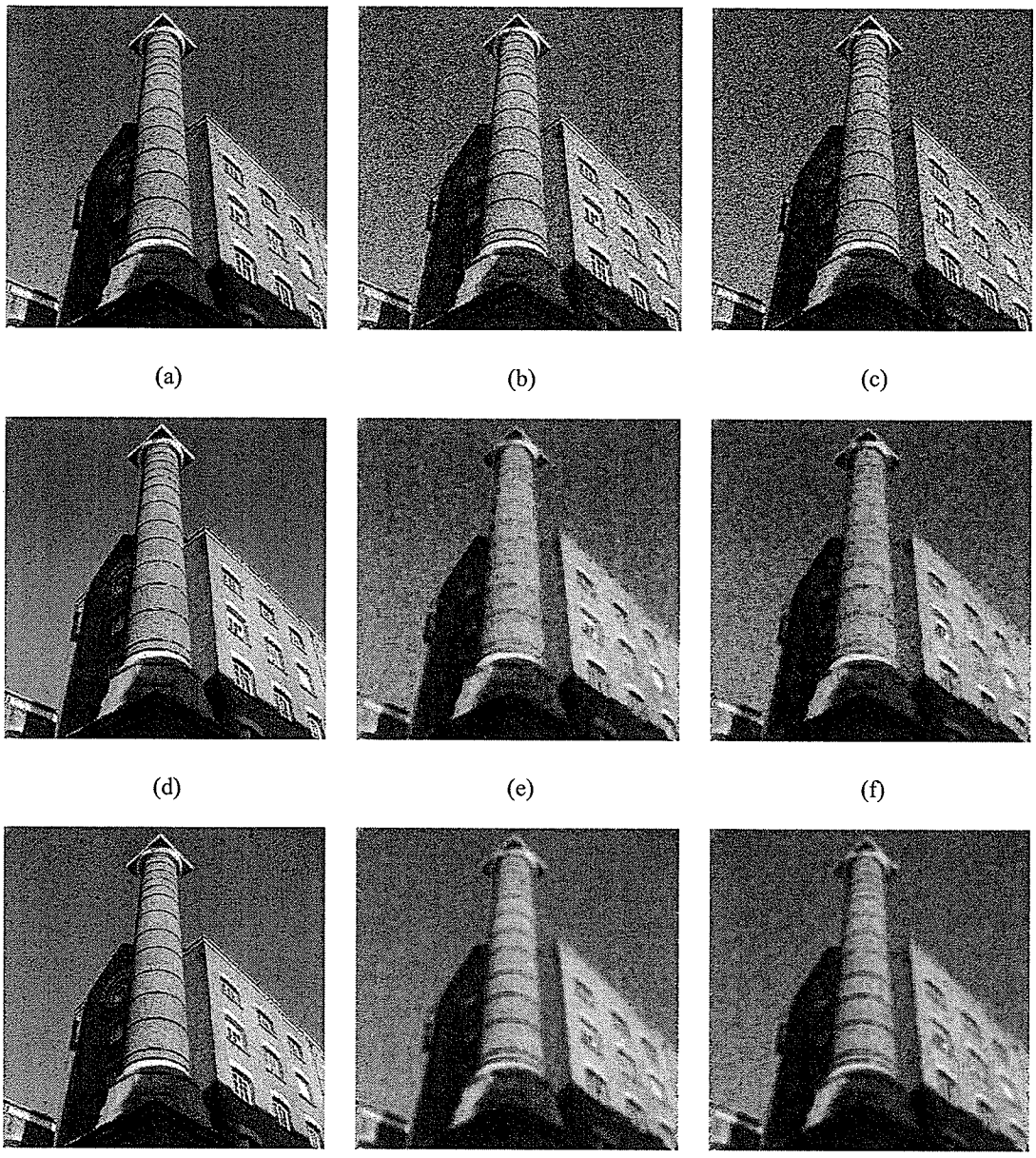

(a) (b) (c)

(d) (e) (f)

(g) (h) (j)

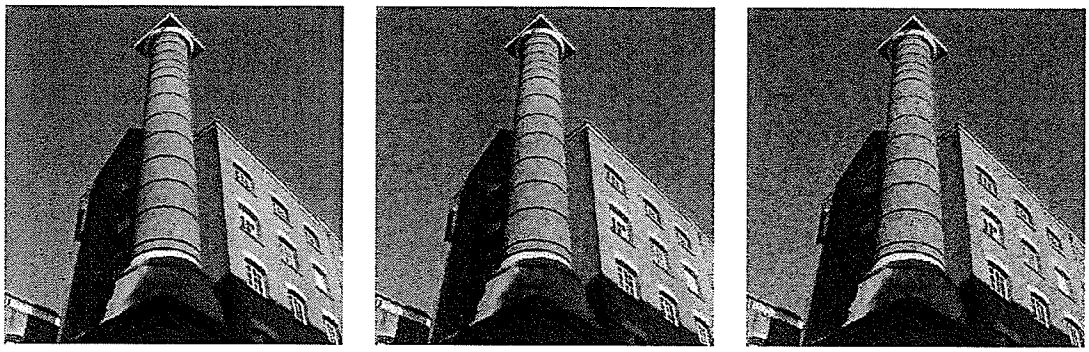

(k) (l) (m)

Figure 4-9 the image corrupted by (a) Impulsive noise, (b) Gaussian noise and (c) mixed impulsive and Gaussian noise. (d) - (f) images recovered by median switch filter, (g) - (i) images recovered by mean switch filter, (j) - (l) images recovered by Sigma filter

The evaluation results show that the best result given by the switch scheme is for the case of impulsive noise -- even the mean switch filter has removed almost all the noise, the sky area is restored to a color of clear blue, and the thin line details on the building is also preserved. In the case of Gaussian noise, the Sigma filter yields a more favourable noise reduction result, while the mean switch filter seconds with slight lag especially in terms of NCD. The median based switch filter did the worst because the median filter's advantage is to suppress short tail noise. Though it still shows a strong performance along the edges of large blocks, the detailed structures of the image has been smeared and artificial patterns are produced. In the case of mixed impulsive and Gaussian noise, we can observe that the switch filters can successfully remove the impulsive noise, but similar to the Gaussian noise case, the restored images are not as good as those processed by Sigma filter.

Chapter 5 Conclusions and Future Work

In this thesis, the switch scheme has been proposed to process additive noise in color images. The impulsive detector, which conducts the function of switching, can effectively separate noise and noise-free pixels. Therefore, the switch filters not only have an excellent performance on impulsive noise, but also preserve subtle details such as thin lines and edges in the image.

The extension of the switch filter to color image processing raises some important issues into consideration, one of which is the variance stabilization transformation. The vector representation of color requires vector filtering techniques to incorporate in the framework. The measurement of color difference demands an appropriate distance measurement to be calculated in a suitable color space so that CIE $L^*a^*b^*$ color space is selected. However, the nonlinear transformation between *RGB* color space and $L^*a^*b^*$ color space changes the noise's additivity property. Most of the noise removal techniques, including the switch filter, were developed based on the assumption of additive noise, and this assumption has to be restored in the filter's working color space by the variance stabilization.

The simulation result demonstrates that the switch filters has excellent performance on impulsive noise. Due to the nature of impulsive detector, the switch scheme performs poorly on Gaussian noise. However, the employment of the mean filter in the framework can remedy this weakness, and result in a general purpose filter when the noise is unknown *a priori*. The experiments results of mean switch filter presented in the thesis show that this

combination takes advantage of Gaussian noise removal ability and computational simplicity from the mean filter.

In a summary, the contributions of my thesis are,

- Extended the nonlinear switch filter from greyscale image processing to color image restoration. The scheme is illustrated in Fig. 2.2 of Session 2.4.
- Derived a transformation to stabilize noise variance which becomes signal dependence after color space conversion.
- Demonstrated a nice combination of linear and nonlinear filter to work as a general purpose filter when noise is unknown *a priori*.

Future work on the switch filter scheme for color image processing may be considered in the following aspects.

The switch scheme in this work only applies a simple step function to determine that the output is either the input signal or the filter result. It's possible to utilize more complicated switch algorithm, such as a ramp function, or an iterated switch algorithm [21], to assign weightings to both input value and filter output, so that more accurate result can be obtained.

The switch filter scheme has already demonstrated its strong ability in impulsive noise reduction. It may make further improvement to handle other types of noise provided suitable denoising filter is employed and proper threshold is chosen. The mean switch filter is a good example, but more filters can be evaluated.

Although the variance stabilization transformation is a useful statistical technique that has been applied to various applications, it's newly utilized to the area of color image processing. The transformation formulae are derived based on the approximation of Taylor series. Optimization may be developed to avoid errors introduced by the approximation, as well as the property of the transformation can be analysed further.

References

[1] J. S. Lee, Digital Image Enhancement and Noise Filtering by Use of Local Statistics, IEEE Trans. On Pattern Analysis and Machine Intelligence, 2, 1980, pp. 165-168.

[2] J. S. Lee, Digital images smoothing and the sigma filter, Computer vision, Graphics, and Image Processing, 24, 1983, pp. 255-269.

[3] K. E. Barner, R. A. Gonzalo, Nonlinear Signal and Image Processing: Theory, Methods, and Applications, CRC Press, 2003.

[4] K. E. Barner, A. M. Sarhan, R. C. Hardie, Partition-Based Weighted Sum Filters for Image Restoration, IEEE Trans. Image Processing, Vol. 8, No. 5, 1999, pp. 740-745.

[5] T. Sun, Y. Neuvo, Detail-preserving Median Based Filters in Image Processing, Pattern Recognit. Lett., vol. 15, 1994, pp. 341-347.

[6] J. W. Tukey, Nonlinear (nonsuperposable) methods for smoothing data, in Congr. Res. EASCON, 1974, p.673.

[7] J. W. Tukey, Exploratory data analysis. Menlo Park, CA: Addison-Wesley, 1971.

[8] C. G. Small, A Survey of Multidimensional Medians, Int. Stat. Rev. vol. 58, no. 3, 1990, pp. 263-277.

[9] J. Astola, P. Haavisto, Y. Neuvo, Vector Median Filters, Proc. Of the IEEE, Vol. 78, No. 4, Apr. 1990, pp. 678-688.

[10] C.K. Chu, I.K. Glad, F. Godtliebsen, and J.S. Marron, Edge preserving smoothers for image processing, *JASA*, 442(93), June 1998, pp. 526-541.

[11] S. Zhang, A. Karim, A new impulse detector for switching median filters, IEEE Signal Processing Lett., vol. 9, 2002, pp. 360-363.

[12] D. L. MacAdam, Ed., Selected Papers on Colorimetry-Fundamentals. Bellingham, WA: SPIE, 1993.

[13] R. C. Gonzalez, R. E. Woods, Digital Image Processing (2nd Edition), Prentice Hall, 2002.

[14] Theory of compound colors, in Philos. Mag., vol. 4, no. 7, 1854, pp. 254-264.

[15] J. C. Maxwell, Theory of the perception of colors, Trans. R. Scottish Soc. Arts, vol. 4, 1856, pp. 394-400.

[16] CIE, Colorimetry, CIE Pub. No. 15.2, Centr. Bureau CIE, Vienna, Austria, 1986.

[17] M. S. Bartlett, The use of transformations, Biometrics, 3, 1947, pp. 39-52.

[18] M. H. Hoyle, Transformations – An introduction and a bibliography, Int. Stat. Rev., Vol.41, No.2, 1973, pp. 203-223.

[19] J. Scharcanski, A. N. Venetsanopoulos, Edge detection of color images using directional operators, IEEE Trans. Circuits Syst. Video Technol., vol. 7, no. 2, 1997, pp. 397-401.

[20] R. T. Chin, C. L. Yeh, Quantitative evaluation of some edge-preserving noise-smoothing techniques, Computer vision, graphics, and image processing 23, 1983, pp. 67-91.

[21] Zh. Wang and D. Zhang, Progressive Switching Median Filter for the Removal of Impulse Noise from Highly Corrupted Images, IEEE Trans. Circuits and Systems II: Analog and Digital Signal Processing, Vol. 46, No. 1, Jan. 1999, pp.78-80.